Annales Societatis Geologorum Poloniae (2013), vol. 83: 113–132.

PROVENANCE OF LOWER CRETACEOUS DEPOSITS OF THE WESTERN PART OF THE SILESIAN NAPPE IN POLAND (OUTER CARPATHIANS): EVIDENCE FROM GEOCHEMISTRY

Patrycja WÓJCIK-TABOL & Andrzej ŚLĄCZKA

Institute of Geological Sciences, Jagiellonian University, Oleandry 2a, PL-30-063, Kraków, Poland; e-mails: p.wojcik-tabol@uj.edu.pl, andrzej.slaczka@uj.edu.pl

Wójcik-Tabol, P. & Ślączka, A., 2013. Provenance of Lower Cretaceous deposits of the western part of the Silesian Nappe in Poland (Outer Carpathians): evidence from geochemistry. *Annales Societatis Geologorum Poloniae*, 83: 113–132.

Abstract: The turbiditic to hemipelagic, fine-grained deposits of the Hradiště Formation (Hauterivian, 132 Ma) to the Lhoty Formation (Albian–Cenomanian, 99 Ma) in the western part of the Silesian Nappe (Polish Outer Carpathians) were studied mineralogically and geochemically to determine if the main factors controlling the chemistry of the sedimentary material can be attributed to provenance, or to post-depositional processes. A high degree of weathering of the source rocks is indicated by the chemical index of alteration (CIA) that varies from 75.98 to 89.86, and Th/U ratios (~4 with outliers at 1.85 and >6). The co-occurrence of rounded and unabraded grains of zircon and rutile, the enrichment in Zr and Hf, as well as the high Zr/Sc ratios suggest that the Hradiště and Veřovice Formations contain recycled material. Plots of La/Th *versus* Hf and Th against Sc show that samples occur in the field of felsic and mixed felsic/basic sources. On a ternary La–Th–Sc diagram, all of the sediments studied are referable to the continental island-arc field. The European Plate, as an alimentary area, has a mosaic structure consisting of Cadomian and Variscan elements. The Proto-Silesian Ridge was detached from the continent, because of rifting. Therefore, it could have corresponded to a continental island arc. The concentrations of Fe and trace metals (e.g., Mo, Au, Cu) in the Veřovice Formation and silica and potassium additions to the Veřovice and Lhoty Formations, as well as the fractionation of REE, and Nb, Ta, Zr, Hf, and Y can be explained by the action of basinal brines. The fluids were of hydrothermal origin and/or were released, owing to the dewatering of clay minerals. Diagenetic processes could have exerted a greater influence on sedimentary rock chemistry than the provenance and sedimentary processes. A distinction between primary, terrigenous elements and those changed diagenetically is necessary for the reliable determination of provenance.

Key words: Silesian Nappe, Lower Cretaceous, mineral composition, geochemistry, provenance, diagenesis.

Manuscript received 17 December 2012, accepted 28 October 2013

INTRODUCTION

The source rocks of the turbiditic sediments of the Outer Carpathians have been investigated for many years and are reasonably well defined (e.g., Książkiewicz, 1962; Poprawa *et al.*, 2002; Cieszkowski *et al.*, 2012). The external basins, such as the Silesian, Subsilesian and Skole basins, were supplied generally by SE- and NE-flowing palaeocurrents from the European Platform and the Proto-Silesian Ridge (known earlier as the Silesian Cordillera), which were built of continental crust (Ślączka, 1976; Strzeboński *et al.*, 2009; Ślączka *et al.*, 2012). Exotics of crystalline rocks (gneisses, granites, igneous rocks with a porphyrytic texture, mica schists) and sedimentary rocks, such as: Carboniferous sandstones and coals, Triassic and Jurassic carbonates and Lower Cretaceous (Urgonian-type) limestones (Cieszkowski *et al.*, 2012) indicate that the detritus was delivered from the crystalline basement and its sedimentary cover. This is supported by the heavy minerals assemblage (garnet, rutile, tourmaline, and zircon, as well as apatite, monazite and epidote), which was examined in samples from the sandstones and conglomerates of the turbiditic succession (Wieser, 1948; Unrug, 1968; Burtan *et al.*, 1984; Winkler and Ślączka, 1992; Grzebyk and Leszczyński, 2006). The rounded grains of heavy minerals occur together with unabraded crystals, indicating a provenance from both the crystalline basement and the older sedimentary rocks. Reworking of the siliciclastic material and redeposition is also documented in numerous olistostromes that occurred during every stage in the evolution of the flysch basin (Cieszkowski *et al.*, 2012).

The geochemistry of fine-grained sediments can provide information regarding provenance, as well as the tectonic setting and the palaeo-environmental evolution of sed-

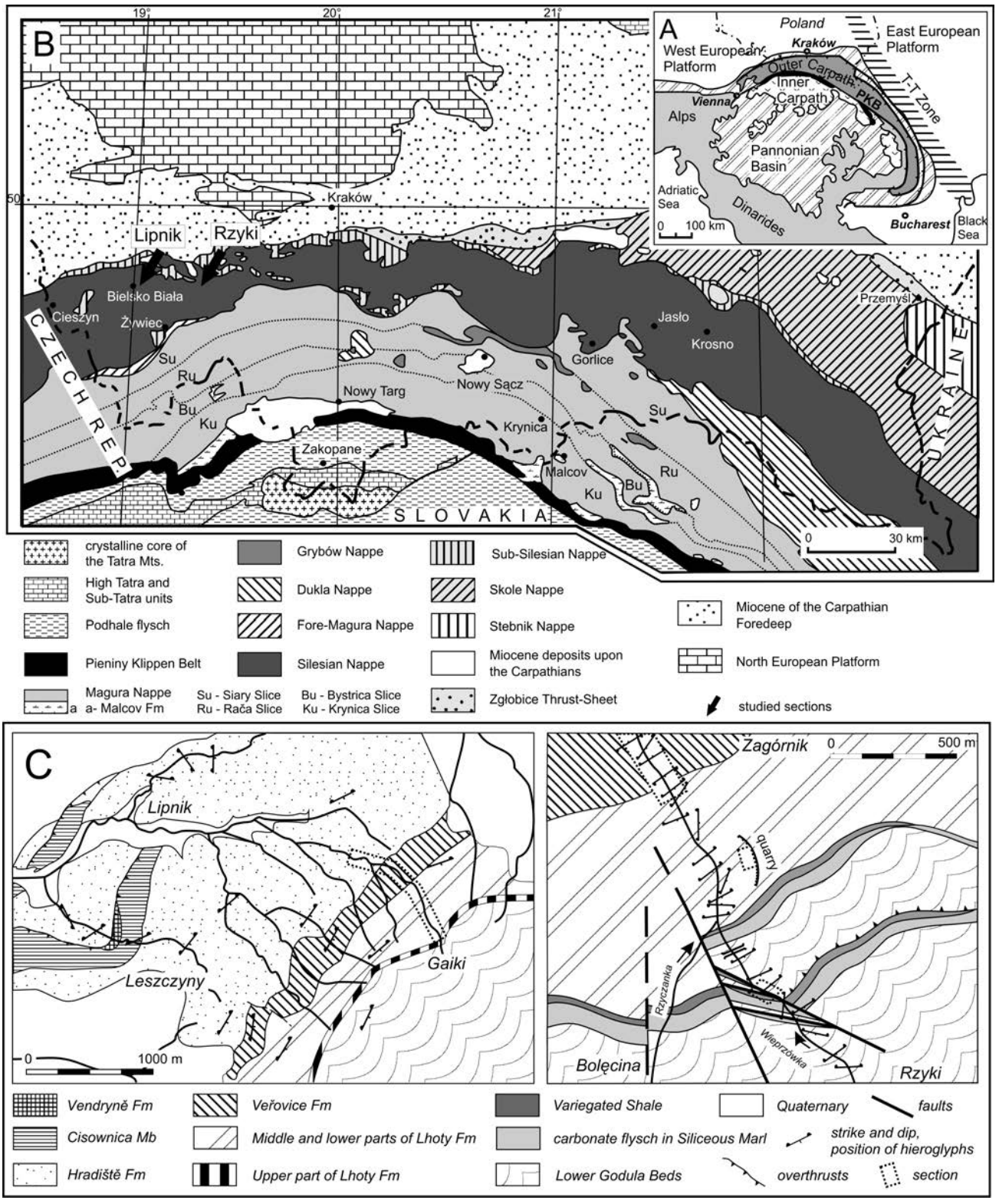

Fig. 1. Location of study area within context of main geological units. **A** – simplified tectonic scheme of Alpine orogens; PKB – Pieniny Klippen Belt (after Kovač *et al.*, 1998, modified); **B** – central part of Polish Carpathians (after Oszczypko & Oszczypko-Clowes, 2009); **C** – Geological map of area around Lipnik (after Geroch & Nowak, 1963; modified) and Rzyki (after Uchman and Cieszkowski, 2008)

imentary basins. The chemical composition of the sediments is a function of several variables, including the nature of the parent rocks, the weathering processes active in the source area, sorting during transportation, reworking of older sediments, as well as sedimentary and post-sedimentary conditions (e.g., Nesbitt and Young, 1982; Johnsson, 1993; McLennan *et al.*, 1993; Fedo *et al.*, 1995). It is necessary to consider the diagenetic processes that involved the alteration of unstable minerals and the precipitation of new phases, usually associated with chemical changes (González-Álvarez and Kerrich, 2010).

The purpose of this study was to characterise and determine the provenance of material, deposited in the Silesian Basin between Hauterivian and Cenomanian times (132–99 Ma according to IUGS 2012). Special attention was given to the fine-grained deposits, the origin of which was determined by means of geochemical data. The geochemical fingerprints of the source rocks were compared to the studies of heavy minerals and the petrology of exotic rocks that have been widely presented by other investigators. This study took into consideration the influence of weathering of the parent rocks and the sorting and recycling of detritus as governing the chemical composition of siliciclastic deposits and changing their chemistry relative to that of the fresh source rocks. Furthermore, diagenetic processes must be taken into account as influencing on the chemical composition of sedimentary rock. This investigation attempted to determine if the main factors responsible for the chemical composition of the material studied are related to provenance, or to post-depositional processes.

Samples were collected from the Lipnik and Rzyki sections, situated in the W part of the Silesian Nappe (Fig. 1). The Lipnik section (Geroch and Nowak, 1963) is located in the E part of the city of Bielsko-Biała and exposes a continuous section from the Cisownica Shale Member (Hauterivian) that represents the lower part of the Hradiště Formation (Golonka *et al.*, 2008) through the Veřovice Formation (Lower Barremian–Lower Aptian, according to Gedl, 2003) and the Lhoty Formation (Albian–Cenomanian), up to the Godula Beds (Turonian) with almost no tectonic disturbance.

In Rzyki village, S of Andrychów, part of the Cretaceous succession is exposed along the stream Wieprzówka (Cieszkowski *et al.*, 2001; Uchman and Cieszkowski, 2008). The profile studied represents the Barremian–Lower Albian Veřovice Formation and the lower part of the Lhoty Formation (Gedl, 2003), strongly tectonized.

GEOLOGY OUTLINE

The Outer Carpathians form the NE part of a great mountain arc, which stretches for more than 1,300 km (Fig. 1A). Structurally, the Outer Carpathians consist of several nappes and thrust sheets: the Magura Nappe, outcropping in the south, the Fore-Magura group of nappes, and the Silesian, Sub-Silesian and Skole nappes, exposed in sequence toward the NE (Książkiewicz, 1968; Kovač *et al.*, 1998; Ślączka *et al.*, 2006). The Outer Carpathian Flysch comprises deep-water sediments, deposited mainly by mass gravity flows and particularly by turbidity currents. The Carpathian tectonic units were thrust from the S on to each other and over the North European Platform (Golonka *et al.*, 2006; Oszczypko *et al.*, 2006).

The study area is situated in the W part of the Silesian Nappe, in the Polish Outer Carpathians (Fig. 1B). Sedimentation in the W part of the Silesian Basin started in the Late Jurassic (Bieda *et al.*, 1963; Ślączka *et al.*, 2006) and began with dark grey, calcareous mudstones (Lower Cieszyn Beds = Vendryně Formation after Golonka *et al.*, 2008) that pass upwards into grey marls and calciturbidites with calcareous, pelagic intercalations of the Tithonian–Beriassian Cieszyn Limestone Formation (Książkiewicz, 1951; Bieda *et al.*, 1963). The clastic material was derived from the adjacent calcareous platforms. The Cieszyn Limestone Formation is covered by dark grey and black, calcareous shales with sideritic mudstone (Upper Cieszyn Shales, equivalent to the Cisownica Shale Member, after Golonka *et al.*, 2008) that represent the lower part of the Hradiště Formation, dated as Valanginian–Hauterivian (after Golonka *et al.*, 2008). Locally, within the upper part of the Hradiště Formation, there are intercalations of thick-bedded sandstones and conglomerates (Piechówka Sandstone Member, after Golonka *et al.*, 2008). In the Barremian part, the calcareous sediments pass upwards into the black shales of the Veřovice Shale, dated as Barremian–Aptian (e.g., Olszewska, 1997) and Barremian–Early Albian (Koszarski and Nowak, 1960; Geroch and Nowak, 1963). In the Bielsko-Biała region, the age of the succession ranges from the Late Barremian to Late Aptian (Gedl, 2003). Golonka *et al.* (2008) proposed the limitation of the Veřovice Formation to the non-calcareous black shales, excluding the lowermost, partly calcareous, black shales that should be assigned to the Hradiště Formation. This sequence records the early stages of development of the Silesian Basin. The latter sequence locally begins with thick-bedded sandstones and conglomerates that pass upwards into thin- and medium-bedded quartzitic sandstones, intercalated with black, greenish shales (the Albian–Cenomanian Lgota Beds of Bieda *et al.*, 1963; the Lhoty Formation after Golonka *et al.*, 2008; Fig. 2B). They represent deposits derived mainly from the northern margin of the basin and from intrabasinal ridges during their uplift and corresponding sea-floor subsidence (Książkiewicz, 1962; Oszczypko, 2006). Deposition in the lower part of the Early Cretaceous occurred during relatively low sea levels and was characterized by a slowing rate of sedimentation from 165 to less than 40 m/My (Poprawa *et al.*, 2006). Deposition of the siliciclastic Lhoty Formation occurred during increases in oceanic level and was accompanied by an acceleration in sedimentation rate (31–63 m/My; Oszczypko, 2006).

This succession is part of the widespread Early Cretaceous Flysch within the Alpine Domain that is characterized by the presence of black, pelitic deposits (Ślączka, 1976; Lemoine, 2003). Usually, these sediments are connected with basins, underlain by oceanic crust, and mark the contact between internal and external zones of the Alpine chains in Europe (Puglisi, 2009). In the case of the external Carpathian basins (Silesian, Subsilesian and Skole basins), the sedimentation of black, pelitic sediments took place during extensional fault movements that embraced the S part of

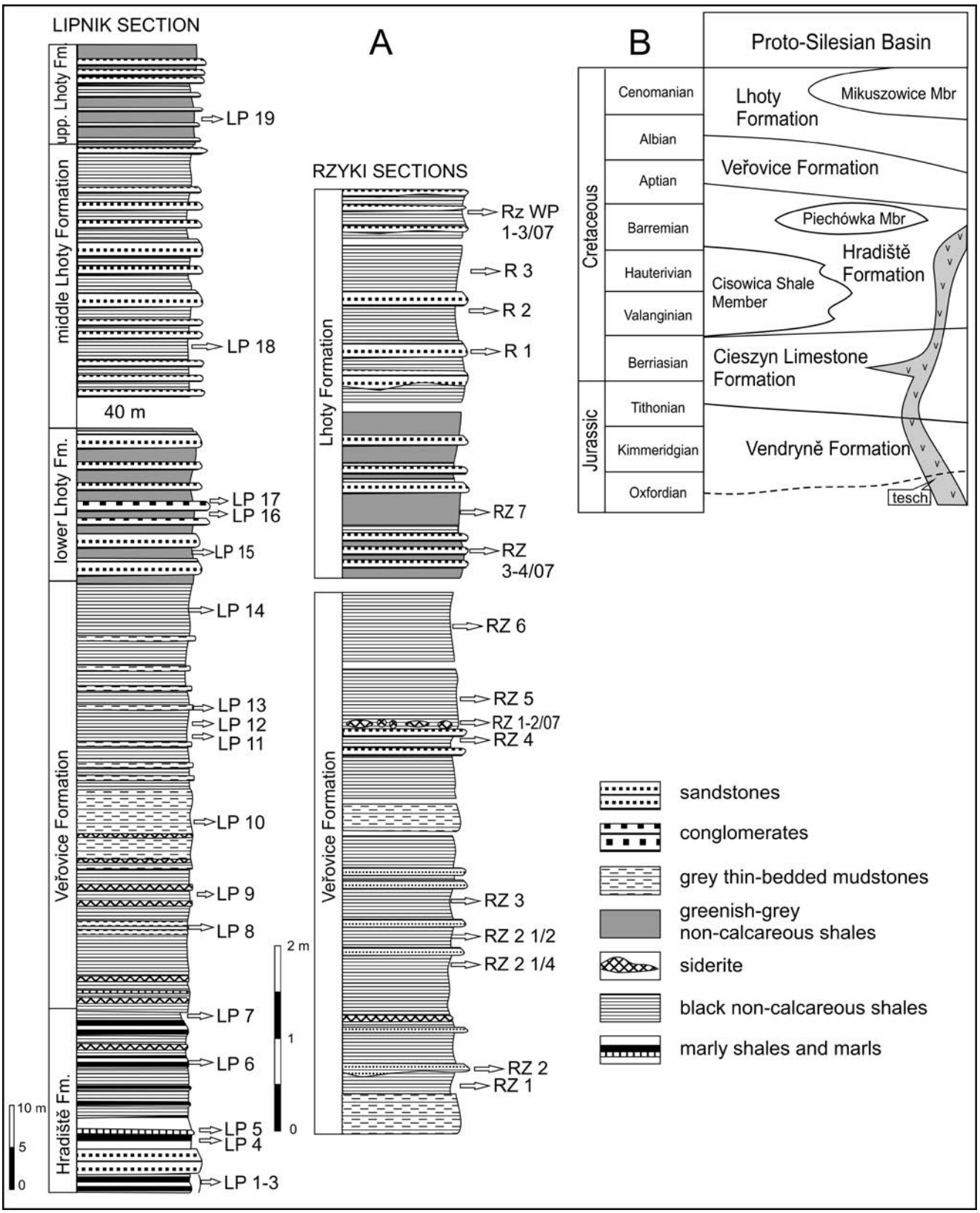

Fig. 2. Lithostratigraphy. **A.** Lithological log of Rzyki and Lipnik sections; **B.** Lithostratigraphy of Jurassic–Cretaceous Proto- Silesian Basin; tesch. – igneous rocks of teschenite association (after Golonka *et al.*, 2008, modified)

Fig. 3. Dark sediments of upper part of Hradiště and Veřovice formations in both studied exposures. **A.** Lower Cretaceous black shales exposed in Lipnik stream; **B.** Wieprzówka stream section. **C.** Dark marly shales interbedded with light grey marls of Hradiště Formation in Lipnik section. **D.** Black shales of Veřovice Formation in Lipnik section. **E.** Fissile black shales with ferrous staining of the Veřovice Formation in Lipnik section. **F.** Black shales intercalated with fine-grained, siliceous sandstones in upper part of Veřovice Formation. **G.** Siderite lenses exposed in Rzyki section (Veřovice Formation). **H.** Burrows filled with fine-grained sandstones in Lipnik section (Veřovice Formation)

the North European Platform. This extensional movement opened and gradually widened the sedimentary basins until the Aptian (Golonka *et al.*, 2006; Oszczypko *et al.*, 2006). Generally, these basins were elongate and narrow (less than 200 km) and 2000–4000 m deep. The Silesian Basin was influenced by magmatism, lasting through 20 Ma from Tithonian/Beriassian to Barremian/Aptian (Ivan *et al.*, 1999; Lucińska-Anczkiewicz *et al.*, 2002; Grabowski *et al.*, 2004; Oszczypko *et al.*, 2012). Hydrothermal activity since the Albian was mentioned by Geroch *et al.* (1985). At the contact with sedimentary host rocks, thermal metamorphism gave rise to hornfels. Igneous bodies and sediments are cut by white to pinkish hydrothermal veinlets. Hydrothermal mineralization is represented by Ca-Fe-Mg carbonates, quartz, chlorite and sulphides (Dolníček *et al.*, 2010, 2012).

Sections studied

The complete section of the Lower Cretaceous part of the Silesian Nappe is exposed in the Lipnik stream, E of Bielsko-Biała (Figs 1C, 3A). The section is 500 m long and exposes continuous sequences from the Cieszyn Limestones Formation to the Godula Beds, with almost no tectonic disturbances, unconformities, hiatuses or repetitions (Fig. 2A; Geroch and Nowak, 1963). The samples labelled LP were collected from the upper part of the Hradiště Forma-

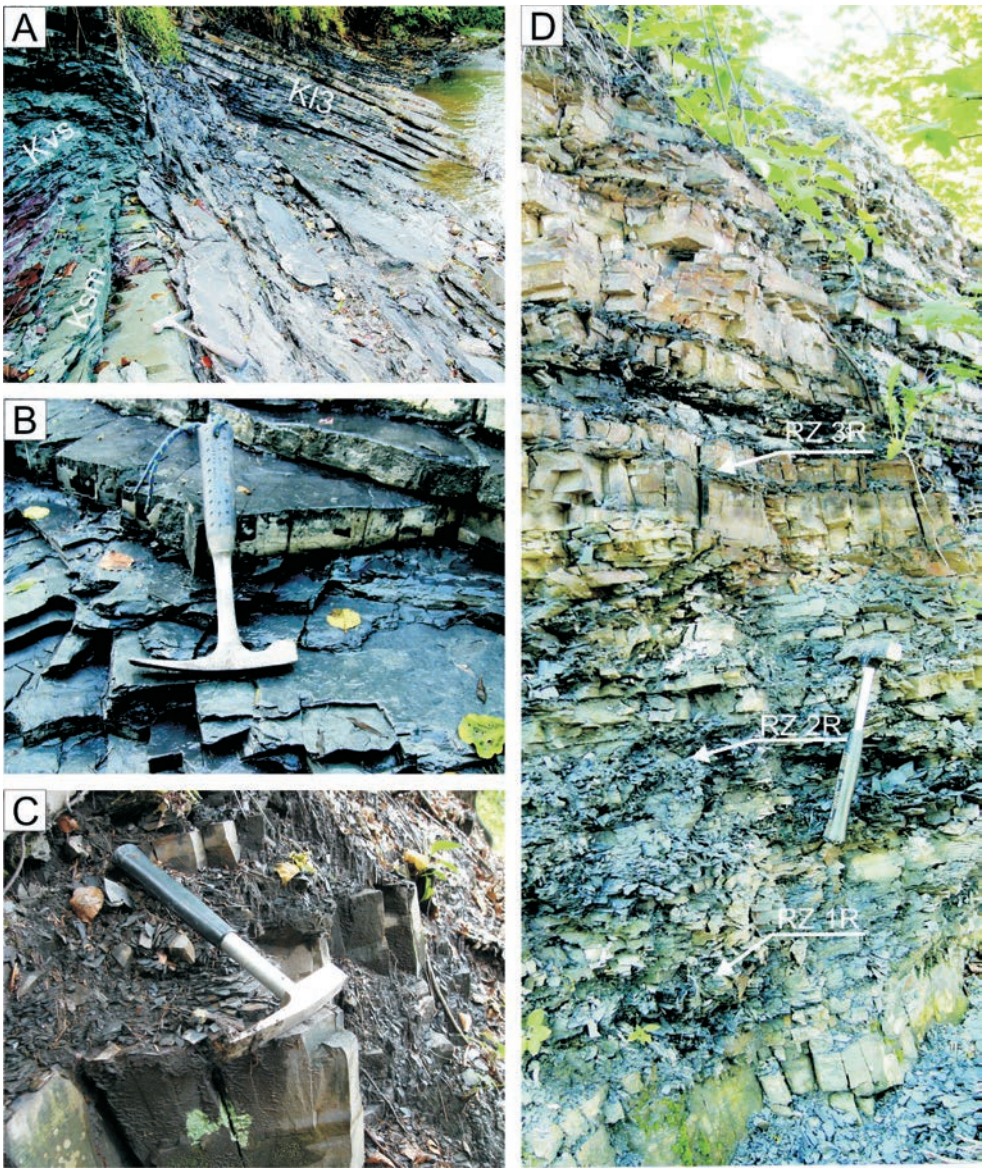

Fig. 4. Lhoty Formation, as seen in Rzyki and Lipnik sections. **A, B.** Uppermost Lhoty Formation at tectonic contact with Variegated Shales in Wieprzówka stream. **C.** Mikuszowice Chert developed as medium-bedded siliceous sandstones with green shales in Lipnik section. **D.** Thin- and medium-bedded, glauconitic sandstones intercalated with grey to black, non-calcareous shales of middle part of Lhoty Formation exposed in quarry near Wieprzówka stream. For explanation, see Fig. 1C

tion, from the Veřovice Formation and from the Lhoty Formation. The Aptian Veřovice Formation and the overlying Lhoty Formation (Albian–Cenomanian; Cieszkowski *et al.*, 2001) are well exposed and were sampled (samples designated R and RZ) along the stream Wieprzówka in Rzyki village, S of Andrychów (Figs 1C, 2A, 3B).

In the Lipnik section, the Hradiště Formation is composed of dark, marly shales, interbedded with light grey shales, and with rare, thin intercalations of grey marls and black, micaeous mudstones (Fig. 3C). This formation gradually passes into the Veřovice Formation. The lowermost part of the Veřovice Formation consists of black, weakly calcareous shales (Fig. 3D). The Veřovice Formation becomes more siliceous up-section and is represented by a succession of non-calcareous, siliciclastic turbidites, including: (1) fissile black shales with ferrous staining (Fig. 3E), interbedded with sideritic mudstone layers (samples: RZ 1–2/07; Fig. 3G), and fine-grained sandstones (sample RZ 2); and (2) hemipelagic, black shales in the upper part of section, intercalated with fine-grained, siliceous sandstones (Fig. 3F–H).

The lower part of the Lhoty Formation in the Lipnik section consists mainly of fine-and coarse-grained, thick-bedded glauconitic sandstones, with intercalations of grey, non-calcareous shales, while the Rzyki section includes only sporadic intercalations of thick-bedded sandstones.

The middle part of the Lhoty Formation consists of bluish grey, thin- and medium-bedded, glauconitic, quartzitic sandstones with parallel lamination and cross-lamination, intercalated with grey to black, non-calcareous shales (Fig. 4D). The upper part of the Lhoty Formation, exposed in the Wieprzówka stream, is developed as thin- to medium-bedded, black, quartzitic sandstones, intercalated with dark grey, fissile shales (Fig. 4A, B).

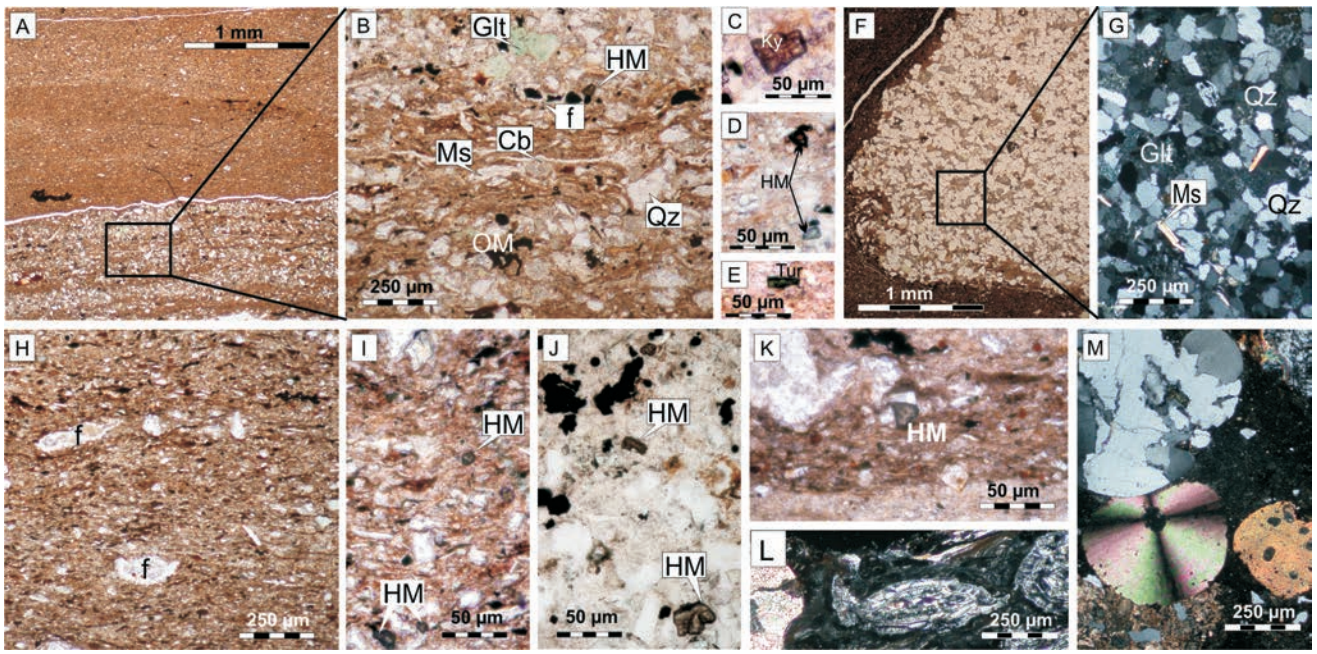

Fig. 5. Microfacies of material studied (all images under transmitted light, in parallel nicols if not stated differently). **A, B.** Mudstones of Hradiště Formation with laminas of fine-grained sandstone (Qz – quartz, Cb – carbonates, Glt – glauconite, OM – organic matter, Ms – muscovite, f – foraminiferids). **C, D, E.** Poorly rounded heavy minerals (= HM) from Hradiště Formation (Tur – tourmaline; Ky – kyanite). **F, G.** Burrows filled with grey, quartzitic sandstones in siliceous shales of Veřovice Formation (G – crossed nicols). **H.** Recrystallised tests of foraminiferids in mudstones of Veřovice Formation. **I, J.** Heavy minerals (= HM) from Veřovice Formation. **K.** Dark bioturbations in green shales of Lhoty Formation. **L, M.** Conglomerate of Lhoty Formation, extraclasts of felsic igneous and metamorphic rocks and limestones containing fragments of echinoderms (crossed nicols)

Green, spotted, fissile shales, intercalated the medium-bedded siliceous sandstones, (Fig. 4C) are typical for the shales of the uppermost part of the Mikuszowice Cherts (upper part of the Lhoty Formation).

ANALYTICAL METHODS

Microfacies were investigated in thin-section, using an optical microscope, the Nikon ECLIPSE, E 600 POL. Every rock sample was hand-pulverised, using a ceramic mortar and pestle, to the fraction passing through a 200-mesh sieve. A classical whole-rock analysis for 11 major oxides (SiO_2, Al_2O_3, Fe_2O_3, MgO, CaO, Na_2O, K_2O, TiO_2, P_2O_5, MnO, Cr_2O_3) by ICP-emission spectrometry followed lithium borate fusion and dilute acid digestion of a 0.2 g sample pulp. ICP-OES analyses of major oxides package included loss on ignition (LOI), which is the weight difference after ignition at 1000°C. Rare earths and refractory elements were reported after lithium borate decomposition to give the total abundances. The amounts of precious metals, base metals and their associated pathfinder elements were obtained from *aqua regia* digestion (ACME Analytical Laboratories, Ltd., 2013). The detection limits and the standards used are given in Table 1.

The major, minor and trace elements in the material studied were compared to those in the standard sediments, Post-Archean Australian Shale (PAAS, after Taylor and McLennan, 1985) and upper continental crust (UCC, after Rudnick and Gao, 2003; Hu and Gao, 2008). The Eu anomaly expressed by the Eu/Eu* ratio was calculated, using $Eu/Eu^* = Eu_N / (Sm_N \times Gd_N)^{0.5}$ ratio, where N is the element content, normalized to UCC. The inter-elemental relationship was evaluated, using Pearson's correlation factor (r). An assumption is that an element positively correlated with Al_2O_3 has a terrigenous derivation. Aluminum is the most important element, which stays inert in biological and diagenetic processes. An additional advantage of using Al is its low abundance in seawater and high concentration in aluminosilicates.

The chemical index of alteration (CIA; Nesbitt and Young, 1982) was used to determine the degree of weathering of the source area. The index is calculated, using molecular proportions in the following equation: $CIA = [Al_2O_3/(Al_2O_3 + CaO^* + Na_2O + K_2O)] \times 100$. The degree of weathering can be presented on an A–CN–K ($Al_2O_3 - CaO^* + Na_2O - K_2O$) triangular plot (Nesbitt and Young, 1984). CaO* is the amount of CaO incorporated in the silicate fraction. If CaO has an affinity to carbonates and LOI is low, and there is no CO_2 and/or P_2O_5, the use of Na_2O as a substitute for ($CaO^* + Na_2O$) is considered to be valid (cf. McLennan, 1993; Hofer *et al.*, 2013). A correction for K enrichment can be made by the projection of lines from the K apex through the data points to the ideal weathering line and reading the value off the CIA axis (Fedo *et al.*, 1995).

RESULTS

Microfacies

The marly shales of the Hradiště Formation contain silt-sized grains of quartz, flakes of phyllosilicates, and indi-

Table 1

Major and trace element geochemistry for Lower Cretaceous deposits recovered from Rzyki and Lipnik sections of Silesian Napp

				Hradiště Formation			Veřovice Formation													Lhoty Formation										PAAS	UCC
	Unit	MDL	STD SO-18	LP 2	LP 4	LP 6	LP 7	LP 8	LP 9	LP 10	LP 12	LP 13	RZ 2 1/4	RZ 3	RZ 4	RZ 1/07	RZ 2/07	RZ 2A/07	RZ 6	RZ 3/07	RZ 7	R1	R2	LP 16	LP 17	LP 18	LP 19	RZ WP 2/07	RZ WP 3/07		
SiO_2		0.01	58.23	56.01	54.86	44.78	51.21	62.41	62.76	65.12	73.81	83.42	67.35	59.95	74.47	73.48	66.44	75.54	60.60	68.84	65.85	64.74	63.42	64.48	72.02	64.46	66.17	67.45	64.06	62.80	63.50
Al_2O_3		0.01	14.57	12.24	7.21	16.21	21.09	14.59	16.29	13.05	11.49	7.19	16.18	18.79	11.02	12.02	9.40	11.90	17.06	12.63	15.91	17.68	16.08	16.72	13.35	17.49	16.31	13.53	14.85	18.90	15.00
Fe_2O_3		0.04	7.49	4.03	1.83	4.74	6.61	5.72	5.45	4.21	2.25	2.24	3.91	4.38	3.47	3.19	7.81	2.87	5.36	3.13	3.75	3.44	4.13	3.49	2.99	3.22	3.92	4.25	4.07	6.50	6.02
MgO		0.01	3.44	1.38	0.83	1.56	1.61	1.54	1.66	1.65	0.91	0.57	1.47	1.51	1.30	1.06	2.49	1.12	1.96	1.95	1.94	1.62	1.50	1.77	1.16	1.32	1.29	1.69	1.96	2.20	3.59
CaO		0.01	6.34	9.13	16.63	12.32	1.67	0.16	0.06	1.29	0.16	0.09	0.11	0.40	0.64	0.28	3.44	0.22	0.97	1.76	0.90	0.78	1.97	0.85	0.23	0.49	0.48	1.46	1.82	1.30	5.25
Na_2O	%	0.01	3.81	0.26	0.20	0.22	0.29	0.52	0.64	0.40	0.42	0.25	0.91	0.91	0.45	0.47	0.45	0.41	0.48	0.30	0.43	0.64	0.59	0.34	0.35	0.32	0.31	0.32	0.26	1.20	3.39
K_2O		0.01	2.18	2.05	1.19	2.04	2.09	2.35	2.65	2.02	1.84	0.83	2.80	3.22	1.97	2.12	1.22	2.16	3.28	3.16	3.70	2.64	2.41	3.92	2.92	3.40	3.03	3.75	4.30	3.70	2.30
TiO_2		0.01	0.69	0.63	0.32	0.67	0.87	0.68	0.77	0.56	0.47	0.39	0.78	0.90	0.47	0.49	0.48	0.49	0.71	0.58	0.68	0.75	0.77	0.73	0.54	0.71	0.62	0.62	0.74	1.00	0.69
P_2O_5		0.01	0.81	0.10	0.07	0.07	0.12	0.09	0.07	0.09	0.08	0.04	0.08	0.09	0.09	0.08	0.09	0.05	0.05	0.07	0.06	0.08	0.07	0.05	0.06	0.07	0.08	0.07	0.10	0.16	0.15
MnO		0.01	0.39	0.03	0.02	0.03	0.03	0.02	0.02	0.03	0.01	<0,1	0.01	0.03	0.02	0.02	0.06	0.02	0.05	0.07	0.03	0.03	0.04	0.02	0.07	0.03	0.04	0.02	0.02	0.11	0.10
LOI		-5.1	1.9	14.10	16.70	17.30	14.20	11.80	9.40	11.40	8.40	4.80	6.40	9.80	6.10	6.70	7.90	5.10	9.50	7.30	6.80	7.50	8.90	7.40	6.10	8.30	7.70	6.80	7.70	nd.	nd.
Na_2O/Al_2O_3				0.02	0.03	0.01	0.01	0.04	0.04	0.03	0.04	0.03	0.06	0.05	0.04	0.04	0.05	0.03	0.03	0.02	0.03	0.04	0.04	0.02	0.03	0.02	0.02	0.02	0.02	0.06	0.23
K_2O/Al_2O_3				0.17	0.17	0.13	0.10	0.16	0.16	0.15	0.16	0.12	0.17	0.17	0.18	0.18	0.13	0.18	0.19	0.25	0.23	0.15	0.15	0.23	0.22	0.19	0.19	0.28	0.29	0.20	0.15
CIA				84.12	83.84	87.76	89.86	82.80	82.94	84.36	82.60	86.00	80.90	80.57	78.27	80.73	84.91	81.01	78.29	78.50	75.98	81.32	84.28	76.59	79.23	80.60	81.02	76.51	76.88	75.30	57.83
Cr_2O_3	%	0.002	0.568	0.012	0.006	0.013	0.017	0.013	0.014	0.014	0.010	0.007	0.017	0.017	0.010	0.011	0.009	0.010	0.015	0.013	0.014	0.013	0.013	0.015	0.01	0.012	0.012	0.012	0.015	nd.	nd.
Cr #				78.95	39.47	85.53	111.84	85.53	92.11	92.11	65.79	46.05	111.84	111.84	65.79	72.37	59.21	65.79	98.68	85.53	92.11	85.53	85.53	98.68	65.79	78.95	78.95	78.95	98.68	110.00	73.00
Co		0.2	23.2	15.00	3.80	11.80	25.80	11.20	6.30	5.90	3.50	1.70	5.20	10.90	17.10	21.90	11.80	7.90	24.90	7.60	6.70	13.60	20.10	6.50	13.00	6.40	11.40	10.60	8.50	23.00	17.30
Sc		1	25	9.00	6.00	13.00	16.00	12.00	15.00	11.00	8.00	6.00	15.00	17.00	11.00	13.00	11.00	10.00	13.00	11.00	15.00	13.00	12.00	15.00	12.00	13.00	12.00	11.00	13.00	16.00	14.00
Hf		0.1	8.5	3.50	2.10	3.80	4.40	4.50	5.30	2.70	2.50	7.70	5.80	5.10	2.60	3.10	4.60	3.00	3.60	2.90	3.50	3.20	3.30	4.00	3.00	3.70	2.70	4.10	4.70	5.00	5.30
Nb		0.1	19.0	13.80	7.30	14.10	18.20	16.50	20.40	11.10	9.90	8.50	18.20	20.50	9.30	10.50	10.90	10.90	15.40	13.10	13.90	14.50	14.40	15.50	10.20	14.70	14.10	13.50	16.10	19.00	12.00
Rb		0.1	26.6	102.00	58.50	92.40	90.80	105.90	107.00	82.60	73.70	33.20	122.00	131.60	79.80	96.80	56.80	100.00	148.10	127.10	154.40	112.30	101.20	168.70	118.00	142.20	119.60	142.20	174.10	160.00	82.00
Sr		0.5	383.0	195.80	280.20	239.40	127.00	86.30	101.80	94.90	68.10	35.50	116.00	163.80	94.90	87.10	102.40	83.40	143.80	113.40	111.10	111.10	127.40	97.10	79.40	97.40	98.40	102.10	119.50	200.00	320.00
Ta		0.1	7.4	0.90	0.50	0.90	1.20	1.10	1.50	0.70	0.70	0.50	1.30	1.40	0.60	0.50	0.50	0.30	1.20	0.50	1.00	1.20	1.10	0.90	0.80	1.10	1.10	0.50	0.80	nd.	0.90
Th		0.2	10.2	9.20	5.60	12.40	15.80	11.30	14.70	7.60	8.60	4.80	13.40	14.50	8.00	8.10	7.70	8.30	13.80	9.70	11.00	14.10	11.20	12.60	9.90	13.20	13.20	10.10	12.50	14.60	10.50
U	ppm	0.1	16.2	2.90	1.70	2.70	3.60	2.90	4.70	3.10	3.40	2.60	3.40	4.00	3.10	2.90	4.00	3.10	2.90	2.20	2.50	2.30	2.60	2.50	2.30	2.40	1.90	2.40	2.70	3.10	2.70
Zr		0.1	263.2	126.10	71.60	133.50	153.50	162.80	176.40	96.80	82.40	305.80	220.80	182.80	88.70	107.60	159.00	89.40	134.80	102.80	130.20	114.40	115.20	137.40	104.00	122.60	99.90	133.60	150.00	210.00	193.00
Y		0.1	33.8	17.60	10.90	19.70	27.30	32.40	42.90	22.00	17.70	16.10	35.00	35.80	19.50	22.90	24.60	14.80	19.40	17.30	19.80	18.10	19.70	19.30	14.70	16.70	17.10	14.10	18.10	27.00	21.00
Mo		0.1	14.5 (1)	0.50	0.20	0.20	1.90	1.10	1.40	1.10	2.20	2.00	0.70	0.70	3.20	2.20	3.50	3.10	0.80	0.30	0.10	0.10	0.20	0.10	0.50	0.10	0.20	0.40	0.20	50.00	1.10
Ag		0.1	1.9 (1)	0.20	0.10	0.10	0.20	0.80	1.00	0.20	0.40	0.30	0.50	0.40	0.60	0.80	0.50	0.30	0.60	0.10	0.10	0.10	0.20	0.10	0.50	0.10	0.10	0.10	0.10	nd.	53 ppb
Au		0.5	109.6 (1)	<0.5	0.60	<0.5	<0.5	0.80	1.00	<0.5	0.90	1.10	6.00	2.90	1.50	0.50	0.50	0.50	1.40	0.50	5.00	9.40	1.10	3.10	2.50	0.90	5.00	0.50	0.50	nd.	1.5 ppb
La		0.1	13.2	27.70	15.60	30.10	33.00	30.20	35.70	28.00	21.90	11.10	32.30	44.00	21.10	25.40	21.90	22.80	34.00	29.10	29.40	26.90	26.80	31.20	32.00	28.00	24.50	24.00	30.60	38.00	31.00
Ce		0.1	29.4	50.40	30.50	65.30	74.60	69.50	91.40	54.00	49.30	26.00	78.60	101.30	47.90	62.90	48.60	48.30	74.30	62.20	65.40	58.70	61.30	68.30	50.70	57.50	52.70	48.40	62.10	80.00	63.00
Pr		0.02	3.53	6.27	3.68	7.16	8.59	8.02	9.81	6.71	5.39	2.96	9.00	11.54	5.60	7.05	5.71	5.40	8.42	7.09	7.18	6.71	6.69	7.76	5.52	6.45	5.95	5.42	6.96	8.80	7.10

MDL – minimal detection limit; 1 – standard STD DS8; Cr # – calculated from Cr_2O_3 according to stoichiometry; N–UCC normalization (Rudnick & Gao, 2003; Hu & Gao, 2008); Ce/Ce* – cerium anomaly calculated using $Ce/Ce^* = Ce_N/(La_N \times Pr_N)^{0.5}$ ratio; Eu/Eu* – europium anomaly calculated using $Eu/Eu^* = Eu_N/(Sm_N \times Gd_N)^{0.5}$ ratio; PAAS according to Taylor and McLennan, 1985; UCC according to Rudnick and Gao (2003), supplemented by Hu and Gao (2008); CIA – chemical index of alteration (after Nesbitt and Young, 1982); nd – no data

	Unit	MDL	STD SO-18	Hradiště Formation				Veřovice Formation												Lhoty Formation								PAAS	UCC
				LP 2	LP 4	LP 6	LP 7	LP 8	LP 9	LP 10	LP 12	LP 13	RZ 2 1/4	RZ 3	RZ 4	RZ 1/07	RZ 2/07	RZ 2A/07	RZ 6	RZ 3/07	RZ 7	R1	R2	LP 16	LP 17	LP 18	LP 19	RZ WP 2/07	RZ WP 3/07		
Nd	ppm	0.3	14.5	23.20	14.10	24.80	35.40	31.50	40.50	25.40	20.60	11.50	35.50	44.80	23.00	29.00	23.70	20.00	32.90	28.10	27.20	24.40	26.20	29.30	18.80	23.90	22.00	20.50	26.50	33.90	27.00
Sm		0.05	3.16	3.50	2.20	4.00	7.00	6.10	7.90	3.80	3.50	2.00	6.90	8.30	4.70	6.51	4.89	3.34	5.20	4.44	4.80	4.60	4.90	4.10	2.80	3.40	4.40	2.94	4.07	5.60	4.70
Eu		0.02	0.95	0.73	0.47	0.88	1.48	1.48	1.78	0.81	0.74	0.41	1.48	1.51	0.97	1.43	1.04	0.69	0.85	0.79	0.91	0.78	0.94	0.81	0.50	0.64	0.70	0.52	0.70	1.10	1.00
Gd		0.05	3.22	2.85	1.92	3.25	5.68	6.37	7.34	3.51	3.01	2.06	6.57	6.13	4.45	6.57	4.98	2.75	3.25	3.56	3.53	3.47	4.10	2.74	1.89	2.35	2.87	2.31	3.32	4.66	4.00
Tb		0.01	0.48	0.50	0.32	0.58	0.96	1.10	1.32	0.59	0.50	0.39	1.16	1.02	0.72	1.01	0.81	0.43	0.56	0.53	0.63	0.59	0.74	0.52	0.35	0.46	0.51	0.41	0.52	0.77	0.70
Dy		0.05	3.19	2.97	1.73	3.74	5.16	6.16	7.87	3.53	3.00	2.44	6.19	5.76	3.80	4.83	4.51	2.60	3.47	3.05	3.55	3.37	3.88	3.28	2.38	2.91	3.11	2.38	3.16	4.40	3.90
Ho		0.02	0.60	0.62	0.35	0.61	0.97	1.13	1.45	0.73	0.55	0.51	1.18	1.14	0.64	0.87	0.84	0.54	0.66	0.62	0.66	0.59	0.68	0.68	0.53	0.60	0.54	0.53	0.66	1.00	0.83
Er		0.03	1.85	1.77	1.02	1.96	2.73	3.30	4.08	2.20	1.75	1.71	3.39	3.56	1.80	2.49	2.59	1.61	2.07	1.82	2.20	1.77	1.89	2.24	1.61	1.75	1.71	1.74	2.08	2.85	2.30
Tm		0.01	0.27	0.25	0.16	0.31	0.39	0.49	0.57	0.33	0.26	0.24	0.54	0.53	0.32	0.37	0.42	0.28	0.35	0.31	0.34	0.29	0.30	0.32	0.25	0.29	0.28	0.31	0.34	0.41	0.37
Yb		0.05	1.72	1.98	1.13	2.01	2.70	3.24	3.92	2.19	1.72	1.77	3.36	3.52	1.79	2.13	2.55	1.72	2.08	1.84	2.15	1.80	1.96	2.37	1.85	1.83	1.73	1.65	2.15	2.80	2.34
Lu		0.01	0.26	0.28	0.16	0.29	0.40	0.47	0.55	0.33	0.28	0.28	0.52	0.53	0.27	0.31	0.39	0.25	0.32	0.28	0.53	0.27	0.29	0.36	0.28	0.29	0.25	0.29	0.31	0.43	0.36
ΣLREE/ΣHREE				13.70	14.06	14.26	12.45	9.64	9.84	12.35	12.96	7.63	10.43	13.55	11.53	11.56	9.15	13.90	16.71	16.01	13.76	14.47	13.44	14.76	15.48	15.04	13.91	14.24	14.56	13.59	
(La/Sm)N				1.20	1.08	1.14	0.71	0.75	0.69	1.12	0.95	0.84	0.71	0.80	0.68	0.59	0.68	1.03	0.99	0.99	0.93	0.89	0.83	1.15	1.73	1.25	0.84	1.24	1.14	1.03		
(Gd/Yb)N				0.84	0.99	0.95	1.23	1.15	1.10	0.94	1.02	0.68	1.14	1.02	1.45	1.80	1.14	0.94	0.91	1.13	0.96	1.13	1.22	0.68	0.60	0.75	0.97	0.82	0.90	0.97		
(La/Yb)N				1.06	1.04	1.13	0.92	0.70	0.69	0.97	0.96	0.47	0.73	0.94	0.89	0.90	0.65	1.00	1.23	1.19	1.03	1.13	1.03	0.99	1.31	1.15	1.07	1.10	1.07	1.02		
Eu/Eu*				1.00	0.99	1.06	1.02	1.03	1.01	0.96	0.99	0.88	0.95	0.92	0.92	0.95	0.91	0.99	0.90	0.86	0.96	0.85	0.91	1.05	0.94	0.98	0.85	0.87	0.83	0.93		
Ce/Ce*				0.90	0.95	1.05	1.04	1.05	1.15	0.93	1.07	1.07	1.09	1.06	1.04	1.11	1.02	1.03	1.03	1.02	1.06	1.03	1.08	1.03	0.90	1.01	1.03	1.00	1.00	1.03		
Rb/Sr				0.52	0.21	0.39	0.71	1.23	1.05	0.87	1.08	0.94	1.05	0.80	0.84	1.11	0.55	1.20	1.03	1.12	1.39	1.01	0.79	1.74	1.49	1.46	1.22	1.39	1.46	0.80	0.26
Nb/Ta				15.33	14.60	15.67	15.17	15.00	13.60	15.86	14.14	17.00	14.00	14.64	15.50	21.00	21.80	36.33	12.83	26.20	13.90	12.08	13.09	17.22	12.75	13.36	12.82	27.00	20.13	nd.	13.33
Th/U				3.17	3.29	4.59	4.39	3.90	3.13	2.45	2.53	1.85	3.94	3.63	2.58	2.79	1.93	2.68	4.76	4.41	4.40	6.13	4.31	5.04	4.30	5.50	6.95	4.21	4.63	4.71	3.89
Zr/Sc				14.01	11.93	10.27	9.59	13.57	11.76	8.80	10.30	50.97	14.72	10.75	8.06	8.28	14.45	8.94	10.37	9.35	8.68	8.80	9.60	9.16	8.67	9.43	8.33	12.15	11.54	13.13	13.79
Zr/Hf				36.03	34.10	35.13	34.89	36.18	33.28	35.85	32.96	39.71	38.07	35.84	34.12	34.71	34.57	29.80	37.44	35.45	37.20	35.75	34.91	34.35	34.67	33.14	37.00	32.59	31.91	42.00	36.42

vidual tests of recrystallized foraminiferids, dispersed in a marly matrix (Fig. 5A). Thin-bedded mudstones display dark trace fossils. The mudstones contain laminae of fine- grained sandstone, composed of quartz, carbonates, layered silicates and scarce grains of glauconite, as well as heavy minerals (i.e. zircon, rutile, tourmaline and kyanite; Fig. 5B–E).

The mudstone and shale microfacies of the Veřovice Formation contain clay and silt fractions with dispersed fine-grained quartz, flakes of phyllosilicates, and glauconite. Scarce microfaunal tests (foraminiferids, radiolaria and sponge spicules) are recrystallized as microcrystalline quartz (Fig. 5H, I). Grains of heavy minerals (i.e. zircon, rutile, tourmaline) are poorly rounded or abraded (Fig. 5I, J). Single rhombohedra of carbonates are visible in the lower part of this formation (Fig. 5I). The matrix is siliceous and darkly colored with organic matter and reddish Fe oxyhydroxides. Some samples of mudstone and shale contain burrows, up to 1 cm in diameter and filled with grey quartzitic sandstone (Fig. 5F, G). Occasionally within the horizons of grey, fine-grained deposits dark ichnofossils occur. Grains of mica, quartz and glauconite are dispersed in the clayey matrix of shales of the Lhoty Formation (Fig. 5K). Horizons, enriched in pyrite concretions, 1 mm in diameter, occur episodically. Coarse-grained layers consist of extraclasts of felsic igneous and metamorphic rocks (chloritoid schists, phyllite, quartzite and hydrothermally altered basic rocks), as well as carbonate bioclasts (Fig. 5L, M).

Geochemistry

Major elements

All samples of fine-grained material in this study are dominated by SiO_2 and Al_2O_3 (Tab. 1). The distribution patterns of major and minor elements, normalized relative to UCC (Rudnick and Gao, 2003) for the material studied, are shown on the Figure 6. The SiO_2 and Al_2O_3 contents in the Lhoty Formation are most similar to those of UCC. The Hradiště Formation is enriched in CaO only (Fig. 6). Generally, the material studied is depleted in most of major and minor elements in comparison to UCC. All samples are strongly depleted in Na_2O. The Lhoty Formation and particular samples of the Veřovice Formation are enriched in K_2O. The samples of the Veřovice Formation that are rich in K_2O also have relatively high TiO_2 and Al_2O_3 content (Fig. 6). Al_2O_3 and TiO_2 are characterized by a strong correlation ($0.84 < r < 0.96$) in all formations, whereas the correlation between Al_2O_3 and K_2O is variable, i.e. coefficient r = 0.6–0.96 with outlier r = –0.4 in the

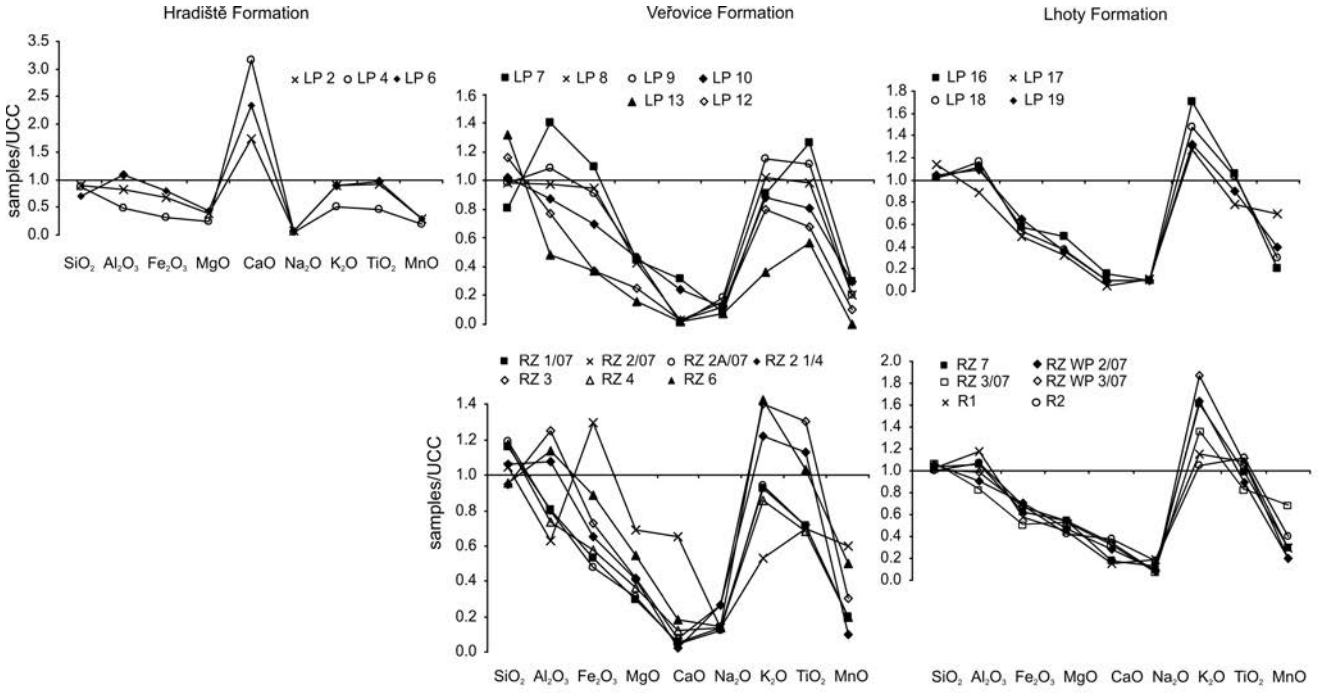

Fig. 6. Spider plots of major and minor elements in Lower Cretaceous deposits of western part of the Silesian Nappe normalized to UCC (Rudnick and Gao, 2003; Hu and Gao, 2008)

Lhoty Formation from the Rzyki (Tab. 2). SiO_2 content is inversely correlated with Al_2O_3, CaO and LOI, as well as with most of oxides of the major and minor elements (Tab. 2). A positive correlation exists between SiO_2 and MnO (r = 0.5), and between MgO and K_2O in the Lhoty Formation from the Rzyki sections (r = 0.7), as well as between SiO_2 and MnO in the Lhoty Formation from the Lipnik section (r = 0.9; Tab. 2).

The concentrations of MgO, K_2O and TiO_2 increase upwards in the rock sequence studied, but Fe_2O_3 and Na_2O reach their highest values in the Veřovice Formation (Tab. 1). A positive correlation of MgO and Fe_2O_3 with Al_2O_3 ($r < 0.5$) occurs in samples from the Lipnik section. In the upper part of the Veřovice Formation, MgO and Fe_2O_3 show a correlation with CaO (r ~0.9; Tab. 2).

The relationship between Na_2O and Al_2O_3 is significantly positive ($0.7 < r < 0.8$) in both formations sampled in the Rzyki section. A reversed correlation of Na_2O with Al_2O_3 (r = –0.7) occurs in the Lhoty Formation at the Lipnik section. In other formations from the Lipnik section, the correlation coefficient is $r < 0.5$ (Tab. 2).

Large ion lithophile elements (LILE): Rb, Sr

Rb reveals a consistently strong, positive correlation with K_2O ($r > 0.9$) and an irregular correlation relative to Al_2O_3. The correlation coefficient is strong (r = 0.76 and 0.93) in the Veřovice Formation from both sections, a moderately positive correlation (r = 0.6) occurs in the Lhoty Formation from the Lipnik section and a weakly negative one typifies the Lhoty Formation from the Rzyki section (r = –0.3). In the Lhoty Formation from the Rzyki section, Rb has a positive correlation with MgO (r = 0.88). Sr is positively correlated with Al_2O_3 ($0.87 < r < 0.97$) in the Veřovice Formation from both sections and in the Lhoty Formation from the Lipnik section. A positive Sr-CaO correlation is common for the material studied ($0.6 < r < 0.99$; Tab. 2). The pattern of multi-elements, normalized to UCC, shows a pronounced Sr depletion (Fig. 7).

High field strength trace elements (HFSE: Zr, Hf, Nb, Ta) and Th, U, REE

The amounts of Zr, Hf in the material studied are lower than those in the UCC, whereas the concentrations of Th, Nb, U, Y and REE are variable (Tab. 1). The strongest enrichment in U, Nb, Ta and REE is noted for samples from the Veřovice Formation (Fig. 8). A positive correlation of Th, Sc, REE with Al_2O_3, K_2O and TiO_2 was commonly recognized in the material studied. The weakest values of correlation coefficient ($r < 0.5$) typify the Lhota Formation from the Rzyki section. The relationship of U relative to Al_2O_3, K_2O and TiO_2 is irregular. The most visible is the correlation of U with K_2O and TiO_2 ($r > 0.4$). Zr and Hf in the Veřovice Formation from the Lipnik section display a negative correlation with Al_2O_3 and a positive one with SiO_2 (Fig. 7, Tab. 2). The samples generally have a low ΣLREE/ΣHREE ratio, ranging from 9.15 to 16.7, with an outlier at 7.6. Many samples record LREE enrichment pronounced in $La_N/Yb_N > 1$. The REE patterns for the Hradiště and Lhoty formations show LREE sloping down to HREE, in some cases with an MREE depletion (Fig. 8) apparent in low Gd_N/Yb_N ratios and $Eu/Eu^* < 1$ (Tab. 1). A few samples from the Veřovice Formation slope upward from La to Lu on the UCC-normalized plots. A convex-up MREE is seen often (Fig. 8). The values of Ce anomaly vary in range

Table 2

Pearson's correlation coefficients (r) between selected major and trace elements for Lower Cretaceous deposits of the Silesian Nappe

Rzyki section, Veřovice Formation																							
	SiO_2	Al_2O_3	Fe_2O_3	MgO	CaO	Na_2O	K_2O	TiO_2	P_2O_5	MnO	Zr	Th	LOI	Rb	Sr	Eu/Eu*	Ce/Ce*	Y	Nb	U	Sc	La	Cr
SiO_2	1.00																						
Al_2O_3	-0.74	1.00																					
Fe_2O_3	-0.55	-0.15	1.00																				
MgO	-0.59	-0.07	0.99	1.00																			
CaO	-0.22	-0.49	0.93	0.89	1.00																		
Na_2O	-0.53	0.75	-0.08	-0.06	-0.34	1.00																	
K_2O	-0.61	0.97	-0.30	-0.21	-0.61	0.59	1.00																
TiO_2	-0.80	0.95	0.01	0.07	-0.33	0.88	0.85	1.00															
P_2O_5	-0.04	-0.17	0.23	0.13	0.28	0.36	-0.34	0.05	1.00														
MnO	-0.53	-0.13	0.90	0.89	0.85	-0.34	-0.20	-0.08	-0.05	1.00													
Zr	-0.66	0.57	0.36	0.38	0.09	0.86	0.38	0.76	0.33	0.04	1.00												
Th	-0.82	0.97	0.02	0.11	-0.34	0.77	0.92	0.97	-0.13	-0.01	0.69	1.00											
LOI	-0.62	0.84	-0.32	-0.27	-0.54	0.34	0.87	0.68	-0.51	-0.03	0.08	0.73	1.00										
Rb	-0.59	0.93	-0.28	-0.18	-0.59	0.51	0.98	0.79	-0.47	-0.16	0.34	0.88	0.87	1.00									
Sr	-0.94	0.87	0.27	0.33	-0.05	0.64	0.77	0.90	0.06	0.29	0.58	0.90	0.77	0.71	1.00								
Eu/Eu*	0.21	-0.56	0.47	0.42	0.61	-0.07	-0.70	-0.33	0.23	0.21	0.23	-0.44	-0.78	-0.68	-0.41	1.00							
Ce/Ce*	0.07	0.37	-0.42	-0.35	-0.52	0.57	0.34	0.42	-0.22	-0.61	0.44	0.38	0.03	0.34	0.04	0.22	1.00						
Y	-0.56	0.58	0.14	0.12	-0.09	0.94	0.39	0.77	0.59	-0.17	0.90	0.63	0.19	0.29	0.59	0.05	0.34	1.00					
Nb	-0.78	0.92	0.04	0.10	-0.29	0.90	0.80	0.99	0.06	-0.08	0.81	0.95	0.62	0.75	0.86	-0.23	0.47	0.81	1.00				
U	-0.48	0.10	0.59	0.54	0.52	0.49	-0.15	0.37	0.60	0.36	0.60	0.19	-0.17	-0.24	0.41	0.56	0.06	0.63	0.42	1.00			
Sc	-0.68	0.85	-0.06	-0.05	-0.35	0.90	0.72	0.91	0.32	-0.18	0.74	0.83	0.69	0.65	0.79	-0.38	0.25	0.88	0.91	0.37	1.00		
La	-0.82	0.95	0.00	0.04	-0.33	0.79	0.86	0.97	0.03	0.00	0.63	0.93	0.83	0.80	0.93	-0.45	0.24	0.70	0.95	0.34	0.92	1.00	
Cr																							

Rzyki section, Lhoty Formation																							
	SiO_2	Al_2O_3	Fe_2O_3	MgO	CaO	Na_2O	K_2O	TiO_2	P_2O_5	MnO	Zr	Th	LOI	Rb	Sr	Eu/Eu*	Ce/Ce*	Y	Nb	U	Sc	La	Cr
SiO_2	1.00																						
Al_2O_3	-0.77	1.00																					
Fe_2O_3	-0.47	0.06	1.00																				
MgO	0.43	-0.48	-0.34	1.00																			
CaO	-0.05	-0.55	0.31	-0.02	1.00																		
Na_2O	-0.53	0.84	-0.09	-0.76	-0.40	1.00																	
K_2O	0.19	-0.43	0.31	0.74	0.05	-0.84	1.00																
TiO_2	-0.99	0.84	0.36	-0.48	-0.05	0.63	-0.29	1.00															
P_2O_5	-0.43	0.08	0.17	0.17	0.29	-0.25	0.37	0.41	1.00														
MnO	0.52	-0.41	-0.74	0.17	0.30	-0.04	-0.44	-0.47	-0.35	1.00													
Zr	-0.35	0.02	0.70	0.31	0.04	-0.46	0.82	0.25	0.53	-0.83	1.00												
Th	-0.68	0.83	-0.05	-0.25	-0.45	0.55	-0.17	0.77	0.56	-0.45	0.19	1.00											
LOI	0.42	-0.57	-0.55	0.52	0.60	-0.36	-0.08	-0.44	-0.19	0.89	-0.49	-0.55	1.00										
Rb	0.09	-0.31	0.25	0.79	-0.01	-0.77	0.98	-0.19	0.40	-0.44	0.83	-0.07	-0.06	1.00									
Sr	-0.67	0.28	0.11	-0.21	0.57	0.29	-0.35	0.64	0.27	0.21	-0.09	0.19	0.37	-0.27	1.00								
Eu/Eu*	0.84	-0.66	-0.05	0.13	-0.09	-0.48	0.28	-0.83	-0.27	0.05	-0.06	-0.53	-0.08	0.13	-0.85	1.00							
Ce/Ce*	0.90	-0.96	-0.24	0.52	0.33	-0.80	0.41	-0.94	-0.13	0.44	-0.11	-0.76	0.51	0.29	-0.48	0.78	1.00						
Y	-0.59	0.59	-0.18	0.02	-0.08	0.48	-0.32	0.60	-0.07	0.16	-0.14	0.33	0.30	-0.15	0.72	-0.91	-0.66	1.00					
Nb	-0.78	0.42	0.39	0.06	0.16	-0.01	0.33	0.75	0.85	-0.56	0.67	0.67	-0.31	0.41	0.49	-0.63	-0.53	0.33	1.00				
U	-0.76	0.25	0.76	-0.02	0.35	-0.08	0.37	0.64	0.43	-0.60	0.74	0.20	-0.25	0.42	0.55	-0.59	-0.47	0.37	0.77	1.00			
Sc	-0.45	0.63	0.00	0.28	-0.60	0.25	0.21	0.45	-0.05	-0.39	0.36	0.45	-0.41	0.36	0.09	-0.56	-0.60	0.67	0.37	0.39	1.00		
La	-0.15	0.00	-0.37	0.74	0.10	-0.30	0.35	0.12	0.36	0.23	0.18	0.15	0.57	0.49	0.43	-0.55	-0.04	0.62	0.45	0.28	0.51	1.00	
Cr	-0.33	0.02	0.43	-0.23	0.45	0.15	-0.21	0.23	-0.42	0.10	-0.03	-0.42	0.28	-0.19	0.60	-0.43	-0.23	0.50	-0.06	0.52	0.13	0.04	1.00

from 0.89 to 1.15, and Eu/Eu* yield values of between 0.82 and 1.06. Only a few samples of the Veřovice Formation show a REE pattern similar to UCC. There is visible, positive correlation of Eu/Eu* with Al_2O_3 (r = 0.3 in the Lhoty Formation, r > 0.8 in the Hradiště and Veřovice formations) in the Lipnik section, whereas an inverse Eu/Eu*–Al_2O_3 correlation (–0.55 and –0.66) occurs for the formation from the Rzyki section. The relationship between Ce/Ce* and Al_2O_3 is not clear. Exceptionally, a clear inverse correlation (r = –0.96) is visible for the Lhoty Formation from the

Table 2 continuation

Lipnik section, Hradiště Formation																							
	SiO_2	Al_2O_3	Fe_2O_3	MgO	CaO	Na_2O	K_2O	TiO_2	P_2O_5	MnO	Zr	Th	LOI	Rb	Sr	Eu/Eu*	Ce/Ce*	Y	Nb	U	Sc	La	Cr
SiO_2	1.00																						
Al_2O_3	-0.77	1.00																					
Fe_2O_3	-0.62	0.98	1.00																				
MgO	-0.62	0.98	1.00	1.00																			
CaO	-0.01	-0.63	-0.78	-0.78	1.00																		
Na_2O	0.28	0.39	0.58	0.58	-0.96	1.00																	
K_2O	-0.41	0.89	0.97	0.97	-0.91	0.76	1.00																
TiO_2	-0.51	0.94	0.99	0.99	-0.86	0.68	0.99	1.00															
P_2O_5	0.58	0.07	0.28	0.28	-0.82	0.94	0.51	0.41	1.00														
MnO	-0.42	0.90	0.97	0.97	-0.91	0.76	1.00	0.99	0.50	1.00													
Zr	-0.51	0.94	0.99	0.99	-0.85	0.68	0.99	1.00	0.40	0.99	1.00												
Th	-0.80	1.00	0.97	0.97	-0.60	0.36	0.88	0.93	0.03	0.88	0.93	1.00											
LOI	-0.71	0.11	-0.11	-0.11	0.71	-0.87	-0.35	-0.24	-0.98	-0.34	-0.23	0.14	1.00										
Rb	-0.22	0.79	0.90	0.90	-0.97	0.88	0.98	0.95	0.67	0.98	0.95	0.76	-0.53	1.00									
Sr	-0.11	-0.54	-0.71	-0.71	0.99	-0.99	-0.86	-0.80	-0.88	-0.86	-0.79	-0.51	0.99	-0.95	1.00								
Eu/Eu*	-0.97	0.90	0.79	0.79	-0.23	-0.04	0.61	0.70	-0.37	0.62	0.70	0.92	0.52	0.44	-0.13	1.00							
Ce/Ce*	-0.97	0.61	0.42	0.43	0.23	-0.49	0.19	0.30	-0.75	0.20	0.31	0.64	0.85	-0.01	0.33	0.89	1.00						
Y	-0.61	0.97	1.00	1.00	-0.79	0.59	0.97	0.99	0.29	0.97	0.99	0.97	-0.12	0.90	-0.72	0.79	0.42	1.00					
Nb	-0.45	0.91	0.98	0.98	-0.89	0.73	1.00	1.00	0.47	1.00	1.00	0.90	-0.30	0.97	-0.84	0.65	0.24	0.98	1.00				
U	-0.27	0.82	0.92	0.92	-0.96	0.85	0.99	0.97	0.63	0.99	0.96	0.80	-0.48	1.00	-0.93	0.49	0.05	0.93	0.98	1.00			
Sc	-0.86	0.99	0.93	0.93	-0.50	0.25	0.82	0.88	-0.08	0.82	0.88	0.99	0.26	0.68	-0.41	0.96	0.72	0.93	0.84	0.72	1.00		
La	-0.55	0.96	1.00	1.00	-0.83	0.65	0.99	1.00	0.36	0.99	1.00	0.94	-0.19	0.93	-0.77	0.74	0.35	1.00	0.99	0.95	0.90	1.00	
Cr	-0.53	0.95	0.99	0.99	-0.84	0.66	0.99	1.00	0.38	0.99	1.00	0.94	-0.21	0.94	-0.78	0.72	0.33	1.00	1.00	0.96	0.89	1.00	1.00

Lipnik section, Veřovice Formation																							
	SiO_2	Al_2O_3	Fe_2O_3	MgO	CaO	Na_2O	K_2O	TiO_2	P_2O_5	MnO	Zr	Th	LOI	Rb	Sr	Eu/Eu*	Ce/Ce*	Y	Nb	U	Sc	La	Cr
SiO_2	1.00																						
Al_2O_3	-0.98	1.00																					
Fe_2O_3	-0.94	0.91	1.00																				
MgO	-0.89	0.81	0.87	1.00																			
CaO	-0.64	0.60	0.48	0.49	1.00																		
Na_2O	-0.26	0.24	0.33	0.53	-0.44	1.00																	
K_2O	-0.77	0.73	0.73	0.88	0.12	0.81	1.00																
TiO_2	-0.95	0.97	0.96	0.82	0.46	0.35	0.76	1.00															
P_2O_5	-0.90	0.86	0.72	0.71	0.76	0.01	0.58	0.73	1.00														
MnO	-0.76	0.59	0.66	0.82	0.84	-0.42	0.08	0.54	0.64	1.00													
Zr	0.46	-0.40	-0.18	-0.51	-0.35	-0.33	-0.60	-0.24	-0.66	0.24	1.00												
Th	-0.88	0.94	0.87	0.73	0.31	0.44	0.78	0.97	0.67	0.26	-0.27	1.00											
LOI	-0.96	0.89	0.85	0.85	0.72	0.15	0.69	0.81	0.97	0.82	-0.58	0.72	1.00										
Rb	-0.81	0.76	0.80	0.89	0.15	0.76	0.99	0.79	0.64	0.16	-0.56	0.80	0.75	1.00									
Sr	-0.98	0.97	0.88	0.90	0.67	0.29	0.78	0.92	0.87	0.80	-0.53	0.87	0.92	0.79	1.00								
Eu/Eu*	-0.82	0.81	0.75	0.77	0.18	0.62	0.92	0.79	0.75	-0.13	-0.63	0.83	0.79	0.95	0.79	1.00							
Ce/Ce*	0.08	0.08	0.06	-0.17	-0.64	0.43	0.17	0.21	-0.34	-0.55	0.37	0.39	-0.33	0.14	-0.09	0.18	1.00						
Y	-0.60	0.61	0.74	0.72	-0.13	0.81	0.83	0.76	0.22	0.10	-0.07	0.77	0.40	0.82	0.59	0.68	0.51	1.00					
Nb	-0.81	0.84	0.90	0.77	0.15	0.59	0.82	0.94	0.49	0.27	-0.11	0.94	0.62	0.83	0.78	0.78	0.45	0.93	1.00				
U	-0.47	0.57	0.43	0.52	-0.03	0.66	0.70	0.62	0.20	-0.10	-0.27	0.74	0.24	0.61	0.58	0.55	0.57	0.76	0.73	1.00			
Sc	-0.95	0.96	0.94	0.88	0.48	0.42	0.81	0.99	0.72	0.61	-0.30	0.95	0.81	0.82	0.95	0.78	0.16	0.79	0.93	0.68	1.00		
La	-0.90	0.88	0.87	0.95	0.35	0.64	0.96	0.90	0.71	0.53	-0.52	0.88	0.81	0.95	0.92	0.89	0.10	0.82	0.89	0.71	0.94	1.00	
Cr	-0.98	0.95	0.90	0.93	0.70	0.28	0.77	0.91	0.88	0.88	-0.51	0.83	0.94	0.79	0.99	0.77	-0.17	0.58	0.77	0.51	0.94	0.91	1.00

Rzyki section. The Ce/Ce*–CaO correlation factor is negative for the Veřovice Formation from both sections and weakly to strongly positive for the Lhoty Formation from both the Rzyki section and the Lipnik section (r = 0.33 and 0.8, respectively).

Diagrams of multi-elements, normalized to UCC (Fig. 7), show positive anomalies for Y relative to Yb in the Veřovice Formation and a slight Y depletion in particular samples from the Lhoty Formation. There are common negative anomalies for Zr–Hf, relative to Nd and Sm. One sample from the Veřovice Formation from the Lipnik section (LP 13) is significantly enriched in Zr–Hf.

TiO_2 shows enrichment relative to Y in the Hradiště and Lhoty formations and depletion in the Veřovice Forma-

Table 2 continuation

Lipnik section, Lhoty Formation																							
	SiO_2	Al_2O_3	Fe_2O_3	MgO	CaO	Na_2O	K_2O	TiO_2	P_2O_5	MnO	Zr	Th	LOI	Rb	Sr	Eu/Eu*	Ce/Ce*	Y	Nb	U	Sc	La	Cr
SiO_2	1.00																						
Al_2O_3	-0.99	1.00																					
Fe_2O_3	-0.53	0.48	1.00																				
MgO	-0.65	0.52	0.28	1.00																			
CaO	-0.80	0.68	0.44	0.97	1.00																		
Na_2O	0.60	-0.67	-0.73	0.13	-0.10	1.00																	
K_2O	-0.72	0.62	0.10	0.95	0.94	0.12	1.00																
TiO_2	-0.94	0.90	0.25	0.78	0.86	-0.29	0.89	1.00															
P_2O_5	-0.09	0.21	0.49	-0.62	-0.43	-0.85	-0.63	-0.24	1.00														
MnO	0.98	-0.93	-0.48	-0.80	-0.91	0.42	-0.85	-0.97	0.12	1.00													
Zr	-0.63	0.55	-0.13	0.87	0.83	0.24	0.97	0.86	-0.70	-0.76	1.00												
Th	-0.94	0.96	0.70	0.41	0.61	-0.83	0.45	0.76	0.42	-0.85	0.32	1.00											
LOI	-0.91	0.97	0.47	0.28	0.47	-0.81	0.40	0.77	0.43	-0.80	0.35	0.96	1.00										
Rb	-0.68	0.58	0.02	0.94	0.91	0.18	1.00	0.87	-0.67	-0.82	0.99	0.39	0.36	1.00									
Sr	-0.96	0.95	0.73	0.53	0.71	-0.77	0.54	0.80	0.31	-0.90	0.41	0.99	0.99	0.49	1.00								
Eu/Eu*	-0.32	0.25	-0.45	0.72	0.61	0.55	0.84	0.63	-0.86	-0.48	0.93	-0.02	0.05	0.88	0.06	1.00							
Ce/Ce*	-0.95	0.91	0.76	0.65	0.80	-0.67	0.62	0.81	0.19	-0.93	0.47	0.95	0.83	0.57	0.98	0.12	1.00						
Y	-0.82	0.71	0.56	0.94	0.99	-0.21	0.88	0.84	-0.31	-0.92	0.75	0.67	0.52	0.84	0.77	0.49	0.87	1.00					
Nb	-0.99	0.95	0.58	0.73	0.87	-0.54	0.77	0.93	0.02	-0.99	0.66	0.91	0.85	0.73	0.95	0.35	0.97	0.89	1.00				
U	-0.16	0.12	-0.66	0.52	0.39	0.62	0.68	0.49	-0.83	-0.29	0.83	-0.17	-0.04	0.74	-0.12	0.97	-0.09	0.26	0.16	1.00			
Sc	-0.61	0.49	0.04	0.97	0.91	0.26	0.99	0.81	-0.73	-0.76	0.96	0.31	0.25	0.99	0.42	0.87	0.53	0.85	0.67	0.72	1.00		
La	0.43	-0.50	-0.78	0.24	0.02	0.97	0.29	-0.09	-0.91	0.25	0.43	-0.71	-0.65	0.35	-0.65	0.72	-0.56	-0.10	-0.39	0.79	0.41	1.00	
Cr	-0.78	0.67	0.44	0.98	1.00	-0.09	0.93	0.85	-0.44	-0.90	0.82	0.59	0.46	0.90	0.70	0.60	0.80	0.99	0.86	0.38	0.91	0.03	1.00

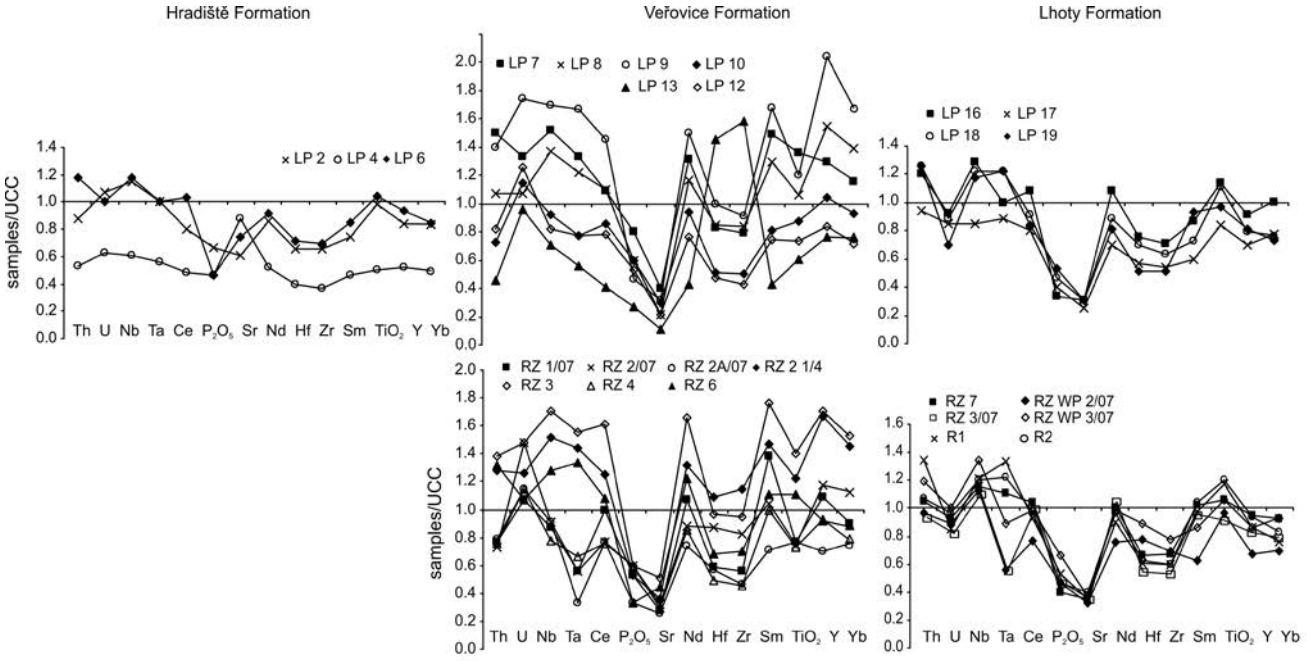

Fig. 7. Spider plots of selected trace elements in Lower Cretaceous deposits of western part of Silesian Nappe normalized to UCC (Rudnick and Gao, 2003; Hu and Gao, 2008)

tion. Variable U/Th ratios stem from a wide range of U concentrations (high in the Veřovice Formation, low in the Lhoty Formation). Positive anomalies of Nb, relative to Ce, and Nb–Ta fractionation, are observed frequently. These features show a general trend to greater decoupling of Ce from P_2O_5, as well as Nb–Ta and MREE from Zr–Hf, and TiO_2 from Y (Fig. 7).

DISCUSSION

Compositional alteration and provenance

The negative correlation of SiO_2 with Al_2O_3 ($-0.98 < r < -0.74$) suggests that quartz grains occur together with siliceous skeletons and diagenetic silica. The presence of radiolarians, sponge needles and agglutinated foraminiferids,

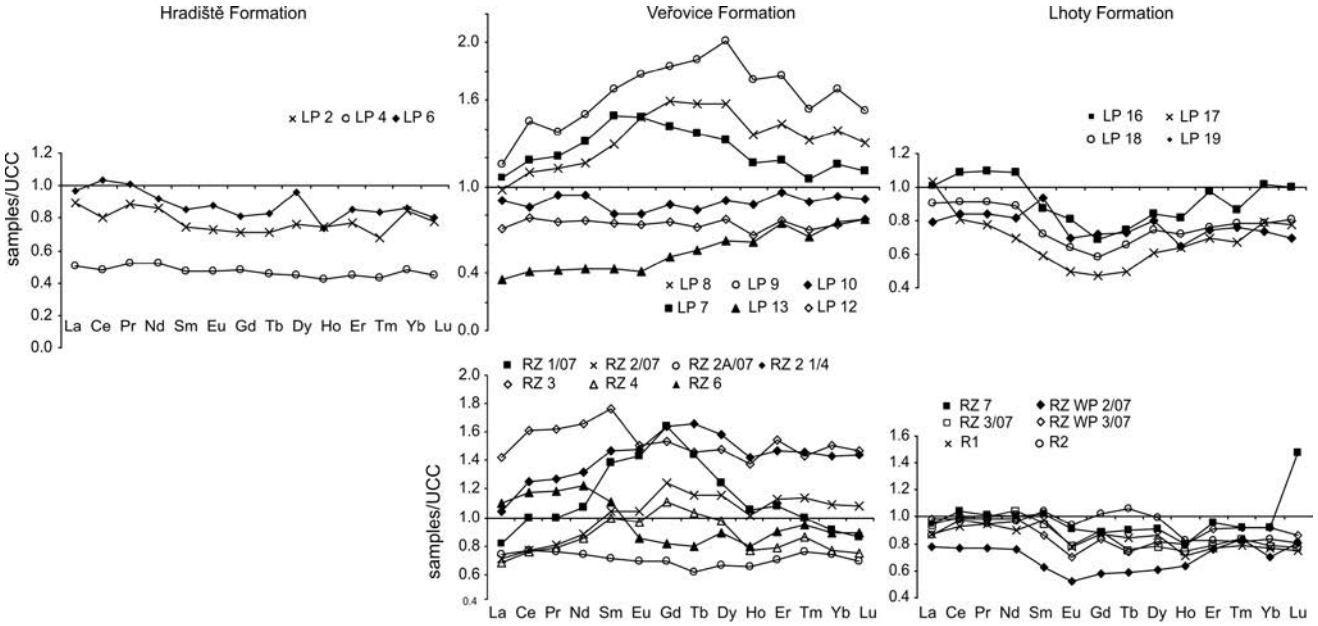

Fig. 8. UCC normalized REE patterns for studied samples

as well as cryptocrystalline quartz, was confirmed microscopically. In general, terrigenous-derived oxides (K_2O, TiO_2, Na_2O) show a positive correlation with Al_2O_3, indicating an important role of mica-type phyllosilicates. However, there are instances of reduced correlation (see the section on major elements) and they are interpreted as the effect of weathering, transport and post-depositional processes. The positive LOI-CaO (Tab. 2) correlation in the Hradiště Formation and Lhoty Formation from the Rzyki section demonstrates that CaO is largely derived from carbonates (Von Eynatten, 2004).

Importance of subaerial weathering

The siliciclastic rocks consist of debris, originating from the decomposition of parent rocks that were affected by a combination of chemical and physical weathering, as well as transport sorting and post-depositional chemical changes. Hydrolytic weathering of unstable minerals, such as feldspar, led to the loss of Na and Ca ions. As weathering continued, K-feldspars should also have been weathered, releasing K (Fedo *et al.*, 1995, 1997; Nesbitt *et al.*, 1997). Finally, it resulted in the formation of clayey deposits, rich in illite and kaolinite, and Fe-oxyhydroxides.

The expected pathways of increasing degrees of weathering for igneous rocks can be traced on the A–CN–K triangular plot (Nesbitt and Young, 1984). Progressive weathering shifts the residual composition towards the Al_2O_3 apex and ever-higher CIA values (Fedo *et al.*, 1995).

In the A–CN–K diagram, the results are located in upper part of triangle, closer to the A–K join (Fig. 9A). The actual trend of the samples differs from the predicted weathering trend (solid arrow). The CIA values of 50 or below are characteristic for unweathered igneous rocks, while residual clays, enriched in kaolinite and Al oxyhydroxides produced under intense weathering, have CIA values close to 100. The CIA values, ranging from 70 to 75 in the typical Phanerozoic shales, reflect muscovite, illite and smectite components and indicate a moderately weathered source (Nesbitt and Young, 1982, 1984; McLennan *et al.*, 1993).

The CIA values calculated in this study vary from 75 to 89 (Tab. 1), whereas CIA for the PAAS and UCC is 75 and 61 respectively. It is necessary to consider the effect of K-enrichment resulting from K-metasomatism or sedimentary incorporation of K-feldspar, suggested by the elevated contents of K_2O, normalized to UCC (see Fig. 6), and the negative correlation of K_2O with Al_2O_3 for the Lhoty Formation from the Rzyki section (Tab. 2). CIA values corrected for potassium-addition vary from 85 to 93.5 (Fig. 9A). Generally, the detritus in the samples is strongly weathered.

The intensity of weathering could be reflected in an increase in the Rb/Sr ratio. Sr is liberated during the decomposition of silicates, whereas Rb is retained in the clay fraction. Therefore, the weathered material is depleted in Sr (Nesbitt *et al.*, 1980; McLennan *et al.*, 1983). Sr depletion in the material studied, excluding the calcareous Hradiště Formation, is pronounced on diagrams of multi-elements, normalized to UCC (Fig. 7). In material studied, Rb displays a stronger affinity to K_2O than to Al_2O_3 (Tab. 2). If the K-feldspathization exerted an influence on the material studied that caused the addition of Rb, then the Rb/Sr ratios would not indicate the degree of weathering of the parent rocks.

The ratio of Th/U can be used as a weathering indicator, because of the low solubility of Th and the oxidation of U^{4+} to the soluble U^{6+} (Taylor and McLennan, 1985; McLennan *et al.*, 1993). The Th/U ratios in the material studied differ from ratio for UCC and PAAS (3.9 and 4.7, respectively; Taylor and McLennan, 1985; Rudnick and Gao, 2003). Outliers at 1.8 and > 6 occur for the Veřovice Formation and

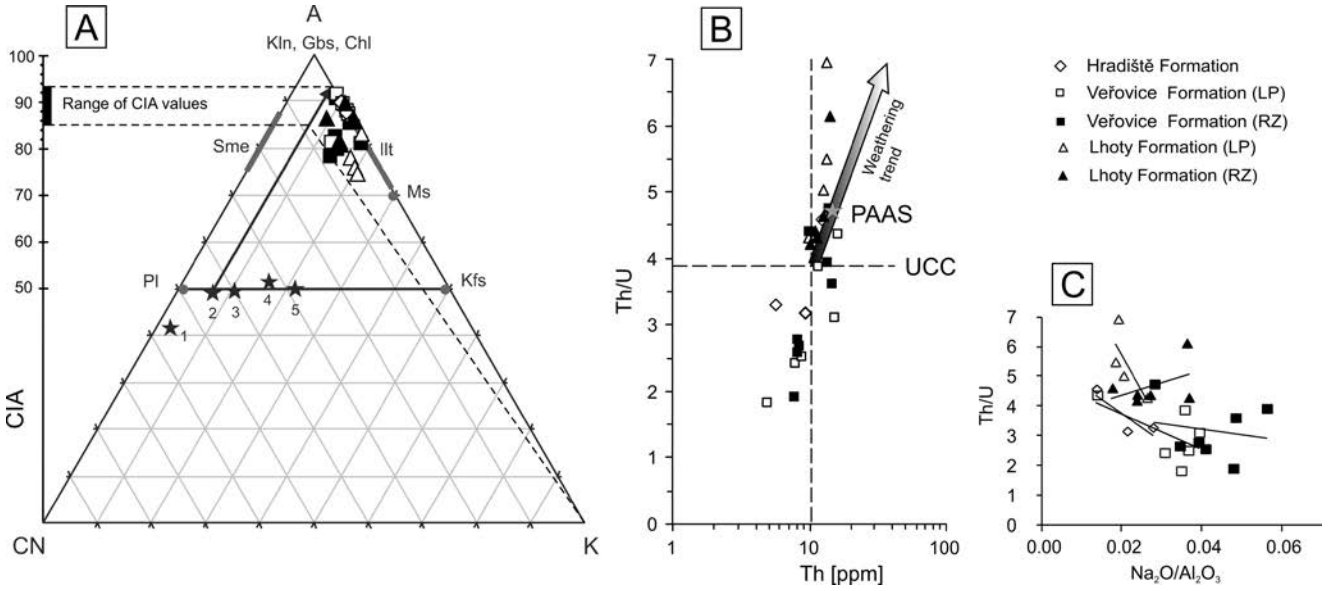

Fig. 9. Weathering indices of detritus in Lower Cretaceous deposits of western part of Silesian Nappe. **A** – Ternary A–CN–K plot of molecular proportions of Al_2O_3–(CaO*+Na_2O)–K_2O for studied material of western part of the Silesian Nappe and chemical index of alteration shown as CIA scale (Nesbitt and Young, 1984). Pl – plagioclase; Kfs – K-feldspars; Ilt – illite; Ms – muscovite; Sme – smectite; Kln – kaolinite; Gbs – gibbsite; Chl – chlorite. Stars: 1 – gabbro; 2 – tonalite; 3 – granodiorite; 4 – granite; 5 – A-type granite from Fedo *et al.* (1997). Solid arrow indicates theoretical weathering trend for tonalite. Correction for K-enrichment can be made by projection of lines from K-apex through data points to ideal weathering line and reading off CIA axis (after Fedo *et al.*, 1995). **B** – Discrimination plot of Th *vs.* Th/U (McLennan *et al.*, 1993). Dashed lines – Th/U and Th content of UCC. Star – PAAS (Taylor and McLennan, 1985). **C** – Th/U *versus* Na_2O/Al_2O_3 diagram

Lhoty Formation, respectively (Tab. 1).The Th/U ratios correlate positively with Al_2O_3, suggesting that the Th/U ratio was not drastically changed during and/or after deposition. The diagram of the relationship of Th/U relative to Na_2O/Al_2O_3 (Fig. 9C) shows that Na_2O/Al_2O_3 and Th/U ratios decrease together in all formations. The graph of Th *vs*. Th/U (Fig. 9B; McLennan *et al.*, 1993) shows that the samples from the Lhoty Formation are more weathered and follow the weathering trend. The black shales of the Hradiště and Veřovice formations that are below the UCC limit have Th/U ratios additionally diminished, owing to the accumulation of U in organic matter and deposition under reducing conditions (McManus *et al.*, 2005). Nevertheless, this reconcentration of U did not disturb the detrital Th/U ratio.

Mineral debris, deposited in the formations studied, was produced by strong chemical weathering, promoted by a warm and humid climate in Late Jurassic–Cretaceous time. This study yields the conclusion that weathering is not the main factor controlling the chemistry of the siliciclastics.

Provenance of detritus

La, Th and Hf tend to be concentrated in silicic rocks more readily than in basic rocks that accommodate Sc, Cr and other compatible elements (Cox *et al.*, 1995; Cullers, 2000). On the basis of its affinity to Al_2O_3, it is inferred that only Th has a detrital derivation in all of the formations studied. A terrigenous origin for La, Sc and Cr can be postulated for the Hradiště and Veřovice formations.

The plot of La/Th *versus* Hf, proposed by Floyd and Leveridge (1987), shows that the samples fall into the field of felsic and mixed felsic/basic sources (Fig. 10A). This corresponds to the diagram of Th against Sc (McLennan *et al.*, 1993) that reveals the continental nature of an alimentary area (Fig. 12B). Samples from the Lhoty Formation do not separate from the others. Thus the influence of depositional and later processes was not significant for the concentration of La and Hf. Ternary La–Th–Sc diagrams (Bhatia and Crook, 1986) were used to determine the provenance and tectonic settings for the deposition of the succession studied. All of the sediments studied occupy the field of continental island arcs (= CIA; Fig. 11).

The Early Cretaceous Silesian Basin was fed by debris originating from the North European Platform, the Baška-Inwałd and Proto-Silesian Ridges, and the Bohemian Massif (Ślączka, 1976; Golonka *et al.*, 2006; Strzeboński *et al.*, 2009). The Baška-Inwałd Ridge and the Proto-Silesian Ridge, as topographically uplifted elements of the North European Platform (Książkiewicz, 1964; Golonka *et al.*, 2006), are exposed parts of the Variscan orogen with late Precambrian (Cadomian) protoliths. The Bohemian Massif is part of the West European plate. It consists of the Variscan orogenic belt and the Cadomian foreland terrane of the Brunovistulicum, composed of metamorphic rocks (Poprawa *et al.*, 2004; Golonka *et al.*, 2006).

In general, the alimentary area was established on continental crust (Sandulescu, 1988; Klomínský *et al.*, 2010). It is evidenced by exotic rocks, such as granites and porphyrites, sericite-chlorite schists, gneisses, and siliciclastics (Cieszkowski *et al.*, 2012 and references therein). Likewise, heavy-mineral assemblages (tourmaline, zircon as well as apatite, monazite and epidote) indicate that non-metamorphic to low-grade metamorphic rocks of granitic continental crust (granitoids, as well as sedimentary pelites and psam-

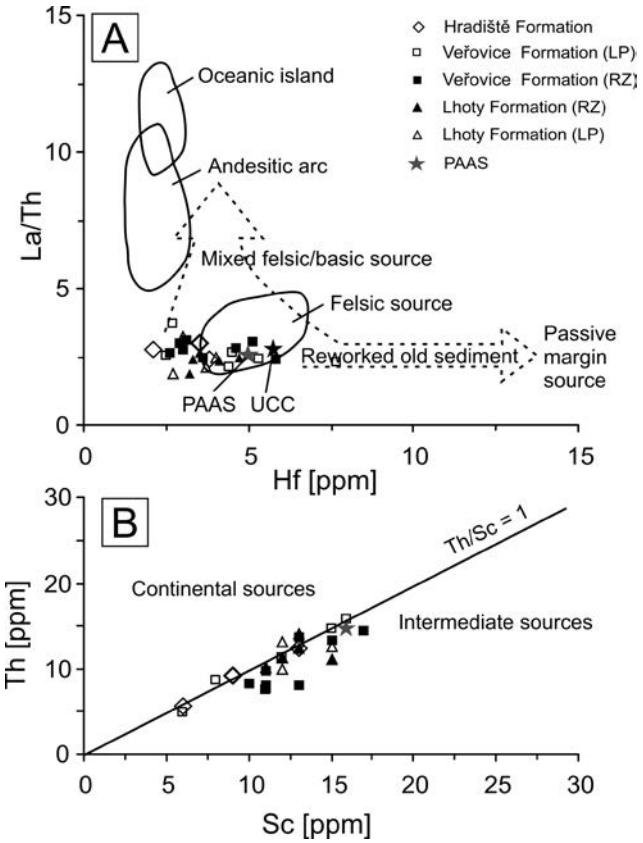

Fig. 10. Discrimination diagrams for provenance of samples studied. **A** – La/Th *versus* Hf diagram (Floyd and Leveridge, 1987); **B** – Th *versus* Sc diagram from McLennan *et al.* (1993)

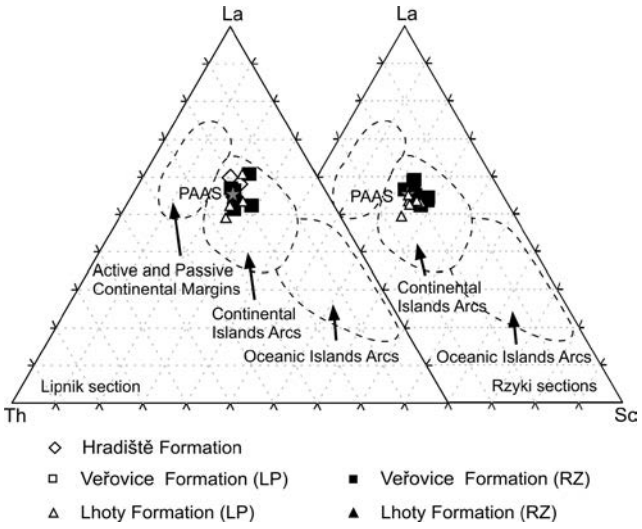

Fig. 11. Discrimination diagram La–Th–Sc for tectonic setting (Bhatia and Crook, 1986)

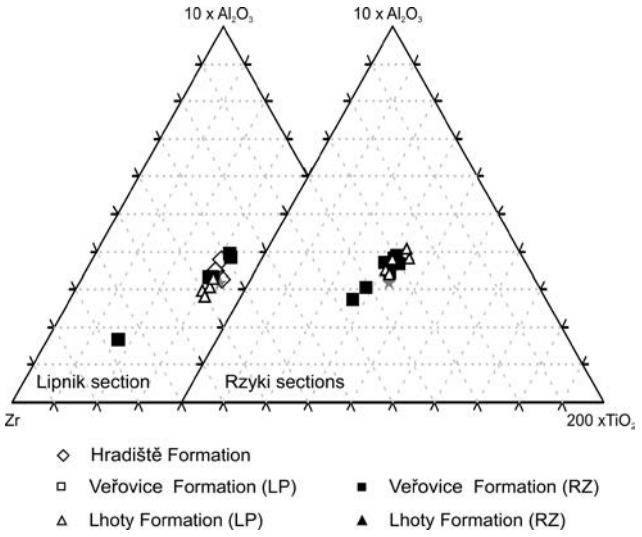

Fig. 12. Ternary 10 x Al_2O_3–200 x TiO_2–Zr plot showing possible sorting trend

mites) were the primary parent rocks for turbiditic deposits in the Cretaceous Silesian Basin.

However, the mosaic structure of the European Plate and the contribution of metamorphic rocks of granulite and partly eclogite facies is reflected in the association of heavy minerals (garnet and rutile; Unrug, 1968; Winkler and Ślączka, 1992; Grzebyk and Leszczyński, 2006). Granulite and eclogite facies typify the conditions of regional metamorphism that act during orogenesis. They can be connected to the old Variscan orogenic belt of the Bohemian Massif. The present studies are in agreement with the published results, because the appropriate heavy minerals were found with kyanite, which is typical for the granulite facies. Moreover, evidence for continental crust as the chief alimentary area was the geochemical signatures and the position of the Carpathian basin as a back-arc basin (Golonka *et al*, 2006; Oszczypko *et al.*, 2006; Puglisi, 2009), bonded to the CIA tectonic province.

Sorting and recycling

Sorting during transportation exerts a major influence on the composition of clastic sediments (Johnsson, 1993; Nesbitt *et al.*, 1997). Gravitational fractionation can result in the separation of quartz and heavy minerals from phyllosilicates. The influence of detrital heavy minerals on geochemistry was tested, using an inverse correlation with Al_2O_3 (Tab. 2). TiO_2 can occur in clay minerals and heavy minerals (e.g. rutile). The most plausible and consistent carrier of Zr and Hf is zircon.

In the material studied, a strong positive correlation between TiO_2 and Al_2O_3 (Tab. 2) suggests an affinity of titanium to phyllosilicates. In the Hradiště and Lhoty formations from the Lipnik section and the Veřovice Formation from the Rzyki section, the TiO_2 concentration parallels those of Zr and Hf (Tab. 2). Thus, the presence of heavy minerals is possible. Nevertheless, the highest concentrations of TiO_2 and Zr occur in samples from the Veřovice Formation (Fig. 7) and the accumulation of heavy minerals is assumed. Zircon can be interpreted as recycled material. The addition of zircon is illustrated on the La/Th *vs*. Hf diagram (Floyd and Leveridge, 1987; Fig. 10B) and on the ternary plot of 10 x Al_2O_3–200 x TiO_2–Zr (Garcia *et al.*, 1991; Fig. 12) The Veřovice Formation falls along a trend involving the addition of zircon. Zircon, rutile and tourmaline form an association of heavy minerals that occur in rewor-

ked material and were recognized in thin-section (see the section on microfacies).

The presence of recycled material within siliciclastic sequences is generally accepted. Veizer and MacKenzie (2003) concluded that about 90% of sedimentary rocks are reworked to produce more sedimentary rocks. The Carpathian successions contain abundant material that underwent several sedimentary cycles. The co-occurrence of rounded and fresh, unabraded grains of heavy minerals suggests a mixed provenance of the clastic material, both from crystalline and older sedimentary rocks (Unrug, 1968; Grzebyk and Leszczyński, 2006). Cieszkowski *et al.* (2012) described the occurrence of olistoliths and olistostromes in many levels of the Silesian Series and also within the Lower Cretaceous sequences of the Hradiště, Veřovice and Lhoty formations, investigated here.

Diagenetic changes

The diagenetic addition of potassium into siliciclastic deposits is widely known (Fedo *et al.*, 1995; Campos Alvarez and Roser, 2007). The post-depositional potassic alteration in fine-grained samples from the Lower Cretaceous sediments of the Silesian Unit is supported by the clayey, illite-rich matrix (Fig. 5), the K_2O enrichment seen on the plots of major element oxides, normalized to UCC (Fig. 6) and the lack of to negative correlation between K_2O and Al_2O_3 (Tab. 2).

The secondary introduction of K into a sediment can be related to the transformation of smectite to illite. Illitization with increasing depth of burial can release certain amounts of water, enriched in Fe and Mg (Bozkaya and Yalçın, 2004), that later play a crucial role during diagenetic processes. González-Álvarez and Kerrich (2010) postulated that the dehydration of the smectite minerals is a likely source of diagenetic brines. The influence of these fluids can be postulated, on the basis of erratic patterns of REE and HFSE distribution.

The analysis of the hydrothermally altered Cretaceous picrite from the Czech Republic led to the conclusion that parent hydrothermal solutions were produced by the dewatering of clay minerals in diagenetically modified flysch sediments (Dolníček *et al.*, 2010, 2012). Therefore, the material studied could have been affected by similar processes.

Mobility of REE and HFSE

REE, Th, Sc and Co are recognized as source-rock indicators (Taylor and McLennan, 1985) and can be mobile under certain conditions of a sedimentary system. Diagenesis at the sediment-water interface, decomposition of the unstable detritus (e.g. volcanic debris), or detrital/biogenic dissolution allow the fractionation of trace elements (Abanda and Hannigan, 2006; McLennan *et al.*, 2006).

Certain samples (Lhoty Fm.: LP 16, RZ WP 2/07, RZ WP 3/07, RZ 3/07; Veřovice Fm.: RZ 1/07, RZ 2/07, RZ 2A/07) have enrichment in Nb, relative to Ta (Fig. 7). Values of the Nb/Ta ratio are between 12.8 and 27, with one outlier at 36.3, whereas UCC ratios = 13.3 (Rudnick and Gao, 2003). This indicates that certain horizons within the sedimentary profile studied were influenced by Nb-rich fluids.

The Zr budget was probably controlled by zircon, which can maintain Zr/Hf ratios through geological processes, such as weathering, transportation, diagenesis and metamorphism. Zr/Hf ratios, ranging from ~35 to ~70, typify an igneous origin of zircon (Murali *et al.*, 1983; Belousova *et al.*, 2002). Nonetheless, hydrothermal or authigenic processes can exert an influence on zircon and cause the fractionation of trace elements (Hoskin, 2005). In the material studied, the Zr/Hf ratios are between 29.8 and 39.7, indicating Zr depletion at particular levels (e.g., the upper part of the Veřovice Formation in the Rzyki section – RZ 2A/07; the upper part of the Lhoty Formation in the Rzyki section – RZ WP 2/07, RZ WP 3/07). The high correlation coefficient ($r > 0.8$) of Zr, relative to K_2O, in the Lhoty Formation indicates post-depositional alteration of the Zr content. An REE distribution lying far away from the UCC pattern reflects the influence of post-depositional processes. Samples from the Rzyki section have a negative Eu/Eu* – Al_2O_3 correlation that indicates diagenetic Eu depletion. The REE fractionation indicated by La_N/Yb_N does not strictly depend on Al_2O_3 and permits the inference that the REE pattern was changed during diagenesis.

Positive Ce anomalies typify most of material studied. The negative anomalies of Ce in the Hradiště Formation are associated with calcite and inherited a Ce depletion similar to that of seawater. Higher values of Ce/Ce* occur in the Veřovice Formation, particularly in samples from the Rzyki section. This could be explained by the scavenging of less soluble Ce^{4+} by suspended particles that settled through the water column (Sholkovitz *et al.*, 1994) or Ce adsorption on Fe-Mn minerals (Elderfield *et al.*, 1990).

The fractionation of REE and Zr-Hf could have been caused by diagenetic processes that involved basinal brines. González-Álvarez and Kerrich (2010) concluded that HFSE and HREE are mobile in oxidized alkaline brines. In fluids with a high pH, REE (preferentially HREE) have an affinity to dicarbonate complexes. Carbon dioxide can be generated by the degradation of organic matter or during the volcanic outgassing, associated with rifting.

The birth of the Outer Carpathian basin was as a result of the European margin rifting in the Late Jurassic–Early Cretaceous (Golonka *et al.*, 2006; Oszczypko, 2006; Ślączka *et al.*, 2006). During the Early Cretaceous time oceanic-crust has been extended (Larson, 1991). The rifting of the European Platform was a main factor controlling the regional subsidence of the Silesian Basin, and accompanied by the mafic volcanism (Ivan *et al.*, 1999; Lucińska-Anczkiewicz *et al.*, 2002; Grabowski *et al.*, 2004; Oszczypko *et al.*, 2012). Igneous rocks of the teschenite association are widespread in the area between Hranice in the Czech Republic and Bielsko-Biała in Poland. The magmatic rocks are classified as teschenites, picrites, monchiquites and alkaline basalts and form intrusive veins, submarine extrusions and pillow lavas (Smulikowski 1930; Kudělásková, 1987; Narębski, 1990). Analysis of the Cretaceous hydrothermally altered picrite from the Czech Republic led to the conclusion that the hydrothermal fluids were released by the diagenetically dewatered clay minerals in flysch sediments (Dolníček *et al.*, 2010, 2012). Therefore, the material studied could have been affected by similar processes.

CONCLUSIONS

Continuous sedimentation of dark turbiditic to hemipelagic deposits in the western part of the Silesian Basin lasted more than 20 Ma, from the Late Jurassic to the Early Cretaceous. The sedimentation of siliciclastics rich in organic matter in the Silesian basin, was controlled by such global events as climatic and CCD changes, as was the case for other black shales (Emeis and Weissert, 2009; Jenkyns, 2010), but also by more local factors, such as the shape of the basin and its evolution, the production of detritus, and sedimentary and diagenetic processes.

The warm and humid climate of Late Jurassic–Cretaceous time promoted chemical weathering. Intense weathering of the source rocks was inferred from Na, Sr, and U depletion, expressed as negative anomalies in multi-elements patterns normalized to UCC, 75.98 < CIA < 89.86 and samples plotting at the A apex on the A–CN–K diagram, and Th/U ratios (~4 with outliers at 1.85 and >6). Heavy mineral associations, including both rounded and unabraded grains of zircon and rutile, enrichment in Zr and Hf, as well as high Zr/Sc ratios suggest that the Hradiště and Veřovice formations contain recycled material.

On plots of La/Th *versus* Hf and Th against Sc, the data occupy the field of felsic material with admixtures from basic sources. The tectonic province of the source area can be determined on the basis of a La–Th–Sc diagram as a continental island arc (CIA). Diagenetic processes could have exerted an influence on the Lower Cretaceous sequences of the Silesian Unit. Concentrations of Fe and trace metals (e.g., Mo, Au, Cu) in the Veřovice Formation and silica and potassium additions in the Veřovice and Lhoty formations, as well as fractionation of REE and Nb, Ta, Zr, Hf, and Y, can be explained as resulting from the action of basinal brines. The fluids were of hydrothermal origin and/or were released, owing to the dewatering of clay minerals. The impact of diagenetic processes on the sediment chemistry is even greater than that of provenance and sedimentary processes.

Acknowledgments

This work was supported by the Polish Ministry of Science and Higher Education (Grant N 307 256139). Many thanks are offered to T. Malata, C. J. Hetherington, and B. Budzyń for critical comments on the first version of the paper, I. Gonzalez-Alvarez for additional remarks and to A. Uchman, F. Simpson and W. Mizerski for linguistic and editorial corrections.

REFERENCES

Abanda, P. A. & Hannigan, R. E., 2006. Effect of diagenesis on trace element partitioning in shales. *Chemical Geology*, 230: 42–59.

Belousova, E. A, Griffin, W. L., O'Reilly, S. Y. & Fisher, N. J., 2002. Igneous zircon: trace element composition as an indicator of source rock type. *Contributions to Mineralogy and Petrology*, 143: 602–622.

Bhatia, M. R. & Crook, K. A. W., 1986. Trace element characteristics of graywackes and tectonic setting discrimination of sedimentary basins. *Contributions to Mineralogy and Petrology*, 92: 181–193.

Bieda, F., Geroch, S., Koszarski, L., Książkiewicz, M. & Żytko, K., 1963. Stratigraphia wniechnikh polskikh Karpat . *Biuletyn Instytutu Geologicznego*, 181: 1–174. [In Russian].

Bland, W. & Rolls, D. 1998. *Weathering. An Introduction to the Scientific Principles*. Arnold Publishers, London, 271 pp.

Bozkaya, Ö. & Yalçın, H., 2004. Diagenetic to low-grade metamorphic evolution of clay mineral assemblages in Palaeozoic to early Mesozoic rocks of the Eastern Taurides, Turkey. *Clay Minerals*, 39: 481–500.

Burtan, J., Chowaniec, J. & Golonka, J., 1984. Preliminary results of studies on exotic carbonate rocks in the western part of the Polish flysch Carpathians. *Biuletyn Instytutu Geologicznego*, 346: 147–156. [In Polish, English summary].

Campos Alvarez, N. O. & Roser, B. P., 2007. Geochemistry of black shales from the Lower Cretaceous Paja Formation, Eastern Cordillera, Colombia: Source weathering, provenance, and tectonic setting. *Journal of South American Earth Sciences*, 23: 271–289.

Cieszkowski, M., Gedl, E., Ślączka, A. & Uchman, A., 2001. Stop C2-Rzyki village. In: Cieszkowski, M. & Ślączka, A. (eds), *Silesian & Subsilesian Units. 12th Meeting of the Association of European Geological Societies & LXXII Zjazd Polskiego Towarzystwa Geologicznego, Field Trip Guide.* Polish Geological Institute, Warszawa, pp. 115–118.

Cieszkowski, M., Golonka, J., Ślączka, A. & Waśkowska, A., 2012. Role of the olistostromes and olistoliths in tectonostratigraphic evolution of the Silesian Basin in the Outer West Carpathians. *Tectonophysics*, 568–569: 248–265.

Cox, R., Lowe, D. R. & Cullers, R. L., 1995. The influence of sediment recycling and basement composition on evolution of mudrock chemistry in the southwestern United-States. *Geochimica et Cosmochimica Acta*, 59: 2919–2940.

Cullers, R. L., 2000. The geochemistry of shales, siltstones and sandstones of Pennsylvanian-Permian age, Colorado, USA: implications for provenance and metamorphic studies. *Lithos*, 51: 181–203.

Dolníček, Z., Kropáč, K., Janíčková, K. & Urubek, T., 2012. Diagenetic source of fluids causing the hydrothermal alteration of teschenites in the Silesian Unit, Outer Western Carpathians, Czech Republic: Petroleum-bearing vein mineralization from the Stříbrník site. *Marine and Petroleum Geology*, 37: 27–40.

Dolníček, Z., Urubek, T. & Kropáč, K., 2010. Post-magmatic hydrothermal mineralization associated with Cretaceous picrite (Outer Western Carpathians, Czech Republic): interaction between host rock and externally derived fluid. *Geologica Carpathica*, 61, 4: 327–339.

Elderfield, H., Upstill-Goodard, R. & Sholkovitz, E. R., 1990. The rare earth elements in rivers, estuaries and coastal sea waters: processes affecting crustal input of elements to the ocean and their significance to the composition of seawater. *Geochimica et Cosmochimica Acta*, 55: 1807–1813.

Emeis, K.C. & Weissert, H., 2009. Tethyan-Mediterranean organic carbon-rich sediments from Mesozoic black shales to sapropeles. *Sedimentology*, 56: 247–266.

Eynatten, H., von, 2004. Statistical modelling of compositional trends in sediments. *Sedimentary Geology*, 171: 79–89.

Fedo, C. M., Nesbitt, H. W. & Young, G.M. 1995. Unraveling the effects of potassium metasomatism in sedimentary rocks and paleosols, with implications for paleoweathering conditions and provenance. *Geology*, 23: 921–924.

Fedo, C. M., Young, G. M., & Nesbitt, G. M., 1997. Paleoclimatic control on the composition of the Paleoproterozoic Serpent

Formation, Huronian Supergroup, Canada: A greenhouse to icehouse transition. *Precambrian Research*, 86: 201–223.

Floyd, P. A. & Leveridge, B. E., 1987. Tectonic environment of the Devonian Gramscatho basin south Cornwall: framework mode and geochemical evidence from turbiditic sandstones. *Journal of the Geological Society,* 144: 531–542.

Garcia, D., Coelho, J. & Perrin, M., 1991. Fractionation between TiO_2 and Zr as a measure of sorting within shale and sandstone series (northern Portugal). *European Journal of Mineralogy*, 3: 401–414.

Gedl, E., 2003. *Biostratygrafia i paleoekologia warstw wierzowskich i lgockich jednostki slaskiej polskich Karpat fliszowych na zachód od Raby w świetle badan palinologicznych.* Unpublished Ph.D. thesis, Jagiellonian University, 246 pp. [In Polish].

Geroch, S., Gucwa, I. & Wieser, T., 1985. Manganese nodules and other indications of regime and ecological environment in lower part of the Upper Cretaceous – exemplified by Lanckorona profile. In: Wieser T. (ed.), *13th Congress of Carpatho-Balkan Geological Association: Fundamental Researches in the Western Part of the Polish Carpathians, Guide to Excursion I.* CBGA XIII Congress, Cracow 1985. Geological Institute, Cracow, pp. 88–100.

Geroch, S. & Nowak, W., 1963. Lower Cretaceous in Lipnik near Bielsko, Western Carpathians. *Rocznik Polskiego Towarzystwa Geologicznego*, 33: 241–263. [In Polish, English summary].

Golonka, J., Gahagan, L., Krobicki, M., Marko, F., Oszczypko, N. & Ślączka, A., 2006. Plate-tectonic evolution and paleogeography of the circum-Carpathian region. In: Golonka, J. & Picha, F. (eds), *The Carpathians and their Foreland: Geology and Hydrocarbon Resources. American Association of Petroleum Geologists Memoir*, 84: 11–46.

Golonka, J., Krobicki, M., Waśkowska-Oliwa, A., Słomka, T., Skupien, P, Vašícek, Z., Cieszkowski, M. & Ślączka, A., 2008. Lithostratigraphy of the Upper Jurassic and Lower Cretaceous deposits of the western part of Outer Carpathians (discussion proposition). *Geologia*, 34: 9–31. [In Polish, English summary].

González-Álvarez, I. & Kerrich, R., 2010. REE and HFSE mobility due to protracted flow of basinal brines in the Mesoproterozoic Belt-Purcell Supergroup, Laurentia. *Precambrian Research*, 177: 291–307.

Grabowski, J., Krzemiński, L., Nescieruk, P., Paszkowski, M., Szydło, A., Pecskay, Z. & Wójtowicz, A., 2004. New data on the age of teschenitic roks (Outer Carpathians, Silesian Unit) – results of the K-Ar dating. *Przegląd Geologiczny*, 52: 40–46. [In Polish, English summary].

Grzebyk , J. & Leszczyński, S., 2006. New data on heavy minerals from the Upper Cretaceous–Paleogene flysch of the Beskid Śląski Mts. (Polish Carpathians). *Geological Quarterly*, 50: 265–280.

Hofer, G., Wagreich, W. & Neuhuber, S., 2013. Geochemistry of fine-grained sediments of the upper Cretaceous to Paleogene Gosau Group (Austria, Slovakia): Implications for paleoenvironmental and provenance studies. *Geoscience Frontiers*, 4: 449–468.

Hoskin, P. W. O., 2005. Trace-element composition of hydrothermal zircon and the alteration of Hadean zircon from the Jack Hills, Australia. *Geochimica et Cosmochimica Acta*, 69: 637–648.

Hu, Z. & Gao, S., 2008. Upper crustal abundances of trace elements: A revision and update. *Chemical Geology*, 253: 205–221.

Ivan, P., Hovorka, D. & Méres, S., 1999. Riftogenic volcanism in the Western Carpathian geological history: a review. *Geoline*, 9: 41–47.

Jenkyns, H. C., 2010. Geochemistry of oceanic anoxic events. *Geochemistry Geophysics Geosystems*, 11: 1–30.

Johnsson, M. J. 1993. The system controlling the composition of clastic sediments. In: Johnsson, M. J. & Basu, A. (eds), *Processes Controlling the Composition of Clastic Sediments.* Geological Society of America Special Paper, 285: 1–19.

Klomínský, J., Jarchovský, T. & Rajpoot, G. S. (eds), 2010. *Atlas of Plutonic Rocks and Orthogneisses in the Bohemian Massif.* Czech Geological Survey, Prague.

Koszarski, L. & Nowak, W., 1960. Notes on the age of the Lgota Beds (Carpathian Flysch). *Kwartalnik Geologiczny*, 4: 468–483. [In Polish].

Kovač, M., Nagymarosy, A., Oszczypko, N., Ślączka, A., Csontos, L., Marunteanu, M., Matenco, L. & Marton, E., 1998. Palinspastic reconstruction of the Carpathian-Pannonian region during the Miocene. In: Rakus, M. (ed.), *Geodynamic Development of the Western Carpathians.* Slovak Geological Survey, Bratislava. pp. 189–217.

Książkiewicz, M., 1951. *Objaśnienia arkusza Wadowice. Ogólna mapa geologiczna Polski 1: 50 000*. Państwowy Instytut Geologiczny, Warszawa, 283 pp. [In Polish].

Książkiewicz, M., 1962 (ed.). *Geological Atlas of Poland. Stratigraphic and Facial Problems, 1:600 000, Book 13, Cretaceous and Early Tertiary in the Polish External Carpathians.* Instytut Geologiczny. [In Polish, English summary].

Książkiewicz, M., 1964. On the tectonics of the Cieszyn Zone. A reinterpretation. *Bulletin of the Polish Academy of Sciences*, 12: 251–260.

Książkiewicz, M., 1968. Evolution structurale des Carpathes polonaises. *Mémoires de la Société Géologique de France*, 42: 529–562.

Kudělásková, J., 1987. Petrology and geochemistry of selected rock types of teschenite association, Outer Western Carpathians. *Geologica Carpathica*, 38: 545–573.

Larson, R. L., 1991. Latest pulse of Earth: Evidence for mid-Cretaceous superplume. *Geology*, 19: 547–550.

Lemoine, M., 2003. Schistes lustres from Corsica to Hungary: back to original sediments and tentative dating of partly azoic metasediments. *Bulletin de la. Société Géologique de France*, 174: 197–209.

Lucińska-Anczkiewicz, A., Villa, I. M., Anczkiewicz, R. & Ślączka, A., 2002. $^{39}Ar/^{40}Ar$ dating of alkaline lamprophyres from Polish Western Carpathians. *Geologica Carpathica*, 53: 45–52.

McManus, J., Berelson, W. M., Klinkhammer, G. P., Hammond, D. E., Holm, C., 2005. Authigenic uranium: relationship to oxygen penetration depth and organic carbon rain. *Geochimica et Cosmochimica Acta*, 69: 95–108.

McLennan, S. M., 1993. Weathering and global denudation. *Journal of Geology*, 101: 295–303.

McLennan, S.M., Hemming, D.K. & Hanson, G.N., 1993. Geochemical approaches to sedimentation, provenance, and tectonics. *Geological Society of America, Special Publications*, 284: 21–40.

McLennan, S. M., Taylor, S. R. & Eriksson, K. A. 1983. Geochemistry of Archean shales from the Pilbara Supergroup, Western Australia. *Geochimica et Cosmochimica Acta*, 47: 1211–1222.

McLennan, S. M.,. Taylor, S. R. & Hemming, S. R., 2006. Composition, differentiation, and evolution of continental crust: constrains from sedimentary rocks and heat flow. In: Brown, M. & Rushmer, T. (eds), *Evolution and Differentiation of the Continental Crust.* Cambridge University Press, pp. 92–134.

Murali, A. V., Parthasarathy, R., Mahadevan, T. M. & Sankar Das, M., 1983. Trace element characteristics, REE patterns and partition coefficients of zircons from different geological environments – A case study on Indian zircons. *Geochimica et Cosmochimica Acta*, 47: 2047–2052.

Narębski, W., 1990. Early rift stage in the evolution of western part of the Carpathians: geochemical evidence from limburgite and teschenite rock series. *Geologica Carpathica*, 41: 521–528.

Nesbitt, H. W., Fedo, C. M. & Young, G. M., 1997. Quartz and feldspar stability, steady and nonsteady-state weathering, and petrogenesis of siliciclastic sands and muds. *Journal of Geology*, 105: 173–191.

Nesbitt, H. W., Markovics, G. & Price, R. C., 1980. Chemical processes affecting alkalies and alkaline earths during chemical weathering. *Geochimica et Cosmochimica Acta*, 44: 1659–1666.

Nesbitt, H. W. & Young, G. M. 1982. Early Proterozoic climates and plate motions inferred from major element chemistry of lutites. *Nature*, 199: 715–717.

Nesbitt, H. W. & Young, G. M. 1984. Prediction of some weathering trends of plutonic and volcanic rocks based on thermodynamic and kinetic considerations. *Geochimica Cosmochimica Acta*, 48: 1523–1534.

Olszewska, B., 1997. Foraminiferal biostratigraphy of the Polish Outer Carpathians: a record of basin geohistory. *Annales Societatis Geologorum Poloniae*, 67: 325–337.

Oszczypko, N., 2006. Late Jurassic–Miocene evolution of the Outer Carpathian fold-and-thrust belt and its foredeep basin (Western Carpathians, Poland). *Geological Quarterly*, 50: 169–194.

Oszczypko, N. & Oszczypko-Clowes, M., 2009. Stages in the Magura Basin: a case study of the Polish sector (Western Carpathians). *Geodinamica Acta*, 22: 83–100.

Oszczypko, N., Salata, D. & Krobicki, M., 2012. Early Cretaceous intra-plate volcanism in the Pieniny Klippen Belt – a case study of the Velykyi Kamenets'/Vilkhivchyk (Ukraine) and Biała Woda (Poland) sections. *Geological Quarterly*, 56: 629–648.

Oszczypko, N., Krzywiec, P., Popadiuk, I. & Peryt, T., 2006. Carpathian Foredeep Basin (Poland and Ukraine): Its sedimentary, structural, and geodynamic evolution. In: Golonka, J. & Picha, F. (eds), *The Carpathians and their foreland: Geology and hydrocarbon resources. American Association of Petroleum Geologists Memoir*, 84: 261– 318.

Poprawa, P., Malata, T. & Oszczypko, N., 2002. Tectonic evolution of the Polish part of Outer Carpathian's sedimentary basins – constraints from subsidence analysis. *Przegląd Geologiczny*, 50: 1092–1108. [In Polish, English summary].

Poprawa P., Malata, T., Oszczypko, N., Słomka, T. & Golonka, J., 2006. Analysis of tectonic subsidence and sedyment deposition rate for the sedimentary basins of the Western Outer Carpathians. In: Oszczypko, N., Uchman, A. & Malata, E. (eds), *Palaeotectonic Evolution of the Outer Carpathian and Pieniny Klippen Belt Basins*. Instytut Nauk Geologicznych Uniwersytetu Jagiellońskiego, Kraków. pp. 179–199. [In Polish, English Sumary].

Poprawa, P., Malata, T., Pecskay, Z. & Banaś, M., 2004. Geochronology of crystalline basement of the Western Outer Carpathians' sediment source areas-preliminary data. *Polskie Towarzystwo Mineralogiczne – Prace Specjalne*, 24: 329– 332.

Puglisi, D., 2009. Early Cretaceous flysch from Betic-Maghrebian and Europe Alpine Chains (Gibraltar Strait to the Balkans); comparison and palaeotectonic implications. *Geologica Balcanica*, 37: 15–22.

Rudnick, R. L. & Gao, S., 2003. The composition of the continental crust. In: Holland, H. D. & Turekian, K. K. (eds), *Treatise on Geochemistry*. Elsevier-Pergamon, pp. 1–64.

Sandulescu, M., 1988. Cenozoic tectonic history of the Carpathians. In: Royden, L. H & Horvath, F. (eds), *The Panonian Basin, a Study in Basin Evolution*. *American Association of Petroleum Geologists Memoir*, 45: 17–26.

Sholkovitz, E. R., Landing, W. M. & Lewis, B. L., 1994. Ocean particle chemistry: The fractionation of rare earth elements between suspended particles and seawater. *Geochimica et Cosmochimica Acta*, 58: 1567–1579.

Smulikowski, K., 1930. Les roches eruptives de la zone subbeskidique en Silesie et Moravie. *Kosmos* A 54: 3–4.

Strzeboński, P., Golonka, J., Waśkowska-Oliwa, A., Krobicki, M., Słomka, T., Skupień, P. & Vašíček, Z., 2009. Veřovice Formation deposits during Early Cretaceous sedimentological regimes in the western part of the proto-Silesian Basin (Moravia, the Czech Republic). *Geologia*, 35: 31–38. [In Polish, English summary].

Ślączka, A., (ed.), 1976. *Atlas of Paleotransport of Detrital Sediments in the Carpathian – Balkan Mountain System*. Instytut Geologiczny, Warszawa, 10 pp.

Ślączka, A., Kruglow, S., Golonka, J. Oszczypko, N. & Popadyuk, I. 2006. The general geology of the Outer Carpathians, Poland, Slovakia, and Ukraine. In: Golonka, J. & Picha, F. (eds), *The Carpathians and Their Foreland: Geology and Hydrocarbon Resources. American Association of Petroleum Geologists Memoir*, 84: 221–258.

Ślączka, A., Renda, P., Cieszkowski M., Golonka, J. & Nigro, F. 2012. Sedimentary basins evolution and olistoliths formation: The case of Carpathian and Sicilian regions. *Tectonophysics*, 568–569: 306–319.

Taylor, S. R. & McLennan, S. M., 1985. *The Continental Crust: Its Composition and Evolution*. Blackwell, Oxford, 312 pp.

Uchman, A. & Cieszkowski, M., 2008. Stop 1, Zagórnik – the Veřovice Beds and their transition to the Lgota Beds: ichnology of Early Cretaceous black flysch deposits. In: Pieńkowski, G. & Uchman, A. (eds), *Ichnological Sites of Poland; The Holy Cross Mountains and the Carpathian Flysch*. *The Second International Congress on Ichnology, Cracow, Poland, August 29–September 8, 2008; Pre-Congress and Post-Congress Field Trip Guidebook*. Polish Geological Institute, Warszawa, pp. 99–104.

Unrug, R., 1968. Kordyliera śląska jako obszar źródłowy materiału klastycznego piaskowców fliszowych Beskidu Śląskiego i Beskidu Wyspowego. *Rocznik Polskiego Towarzystwa Geologicznego*, 38: 81–164. [In Polish, English summary].

Veizer, J. & Mackenzie, F. T., 2003. Evolution of sedimentary rocks. In: Holland, H. D & Turekian, K. K. (eds), *Treatise on Geochemistry*, 7. Elsevier-Pergamon, Oxford, pp. 369–407.

Wieser, T., 1948. Egzotyki krystaliczne w kredzie śląskiej okolic Wadowic. *Rocznik Polskiego Towarzystwa Geologicznego*, 18: 109–150. [In Polish, English summary].

Winkler, W. & Ślączka, A., 1992. Sediment dispersal and provenance in the Silesian, Dukla and Magura flysch nappes (Outer Carpathians, Poland). *International Journal of Earth Sciences*, 81: 1437–3254.